Host specialization in microparasites transmitted by generalist vectors: insights into the cellular and immunological mechanisms

Yi-Pin Lin[1,2#]*, Danielle M. Tufts[3#], Alan P. Dupuis, II[1], Matthew Combs[3], Ashley L. Marcinkiewicz[1], Andrew D. Hirsbrunner[1], Alexander J. Diaz[1], Jessica L. Stout[1], Anna M. Blom[4], Klemen Strle[1], April D. Davis[1], Laura D. Kramer[1,2], Maria A. Diuk-Wasser[3]*

[1]Division of Infectious Diseases, Wadsworth Center, New York State Department of Health, Albany, NY, USA, [2]Department of Biomedical Sciences, State University of New York at Albany, NY, USA, [3]Department of Ecology, Evolution, and Environmental Biology, Columbia University, New York, NY USA, [4]Division of Medical Protein Chemistry, Department of Translational Medicine, Lund University, Malmo, Sweden

Short title: Early defense and pathogen adhesiveness confer spirochete host specialization

Key words: Lyme disease, *Borrelia*, Early immune responses, Adhesion

[#]Contributed equally to this work

*correspondence: Yi-Pin Lin, Ph.D.
Division of Infectious Disease,
Wadsworth Center, New York State Department of Health
120 New Scotland Ave., Albany, NY 12047
Telephone: 518-402-2233; Fax: 518-473-1326
Email: Yi-Pin.Lin@health.ny.gov

*correspondence: Maria A. Diuk-Wasser, Ph.D.
Department of Ecology, Evolution, and Environmental Biology,
Columbia University
1200 Amsterdam Ave., New York, NY 10027
Telephone: 212-854-3355
Email: mad2256@columbia.edu

ABSTRACT (289 words)

Host specialization is an ecological and evolutionary process by which a pathogen becomes differentially adapted to a subset of hosts, restricting its host range. For parasites transmitted by generalist vectors, host specialization is not expected to evolve because of the decreased survival of those parasites in inadequate hosts. Thus, parasites may develop adaptation strategies, resulting in host specialization. The causative agents of Lyme disease are multiple species of bacteria, *Borrelia burgdorferi* sensu lato species complex (*Bb*sl), and are suitable for examining host specialization as birds and rodents were found to carry different species of these bacteria. Debate exists on whether host specialization occurs among these strains within a particular species of *Bb*sl, such as *B. burgdorferi* sensu stricto (*Bb*ss). Current evidence supports some *Bb*ss strains are widespread in white-footed mice but others are in non-rodent vertebrates, such as birds. To recapitulate specialization in the laboratory and define the mechanisms for host specialization, we introduced different genotypes of *Bb*ss via tick transmission to American robins and white-footed mice, the Lyme disease reservoirs in North America. Among these strains, we found distinct levels of spirochete presence in the bloodstream and tissues and maintenance by these animals in a host-dependent fashion. We showed that the late stage persistence of these strains largely corresponds to bacterial survival at early infection onsets. We also demonstrated that those early survival phenotypes correspond to spirochete adhesiveness, evasion of complement-mediated killing in sera, and/or not triggering high levels of pro-inflammatory cytokines and antibodies. Our findings thus link host competence to *Bb*ss with spirochete genotypic variation of adhesiveness and inducing/escaping host immune responses, illuminating the potential mechanisms that dictate host specialization. Such information will provide a foundation for further investigation into multi-disciplinary processes driving host specialization of microparasites.

AUTHOR SUMMARY (200 words)

Host specialization arises when microparasites adapt to a subset of available hosts, restricting the host ranges they can infect. The mechanisms and selective pressures for the evolution of host specialization remain unclear. The causative agent of Lyme disease (LD), the bacteria species complex of *Borrelia burgdorferi* sensu lato, is adapted to different vertebrates. However, whether such a differential host adaption also applies to each genotype within the same species is under debate. Further, the mechanisms that drive such host specialization are unclear. We thus introduced three genotypes of one LD bacteria species (*B. burgdorferi* sensu stricto) individually via tick bite to American robins and white-footed mice, the most common LD reservoirs in North America. We found that these genotypes differed in the persistent maintenance by those reservoirs and occurred in a host-specific fashion. The ability of those bacteria for long-term maintenance was linked with their capability to attach to cells and a lack of induction of high levels of immune responses at early infection onsets. This work demonstrates the potential mechanisms that dictate host specialization of LD bacteria circulating in natural populations. Such information will pave the road to define the molecular, ecological, and evolutionary determinants that drive host-microparasite interactions.

INTRODUCTION

The range of hosts a parasite can infect is arguably one of the most important properties of a parasite because it can determine, among other things, whether a parasite can survive the extinction of a host species and whether it can become established and spread following its introduction to a new area (1, 2). Host specialization is defined as the ecological and evolutionary process by which a pathogen becomes differentially adapted and thus restricts its host range to a subset of potential hosts. For vector-borne microparasites, such a process is expected to evolve when vectors are specialized to competent hosts, leading to microparasite amplification. However, it is much less obvious how and when host specialization in a vector-borne microparasite can occur and when vectors are host-indiscriminate. Given the significant cost incurred when microparasites are inoculated into incompetent hosts, the evolution of host specialization is only expected to occur when it provides a significant selective advantage for the microparasite to overcome cellular or immunological barriers to infection.

The spirochetes of the *B. burgdorferi* sensu lato (s.l.) species complex, agents of Lyme disease, represent an ideal system to investigate the tradeoffs involved in the evolution of host specialization. *B. burgdorferi* s.l. is maintained in an enzootic cycle between generalist ticks of the *Ixodes ricinus* complex and reservoir hosts, including small and medium-sized mammals, birds, and reptiles (3-5). Despite being transmitted by the same generalist vector, some *B. burgdorferi* s.l. genospecies in Europe are almost exclusively associated with a host taxa (e.g. *B. afzelii* in rodents; *B. garinii* in avian hosts). In contrast, *B. burgdorferi* sensu stricto (hereafter *B. burgdorferi*) in North America is considered a host generalist as it has been isolated from multiple classes of vertebrate animals including mammalian and avian hosts (3, 6-8). However, laboratory infection studies indicate that the fitness of *B. burgdorferi* strains varies in different hosts (9, 10).

97 In natural populations, weak associations were also found between hosts and particular *B.*
98 *burgdorferi* genotypes, defined by polymorphic markers, such as *ospC* or 16S-23S rRNA
99 intergenic spacer type (RST) (11-13). An intriguing possibility is that the partially and regionally
100 constrained host associations observed in *B. burgdorferi* genotypes represent an incipient
101 evolutionary process of host specialization (4, 12, 14-17). That is, *B. burgdorferi* may be on an
102 evolutionary path to diversify into host specialized genospecies, similar to those within the *B.*
103 *burgdorferi* s.l. species complex in Europe. Nonetheless, the molecular processes underlying such
104 diversification and the extent to which they might drive genome-wide diversification in *B.*
105 *burgdorferi* remain under debate.

106 Multiple-niche polymorphism (MNP), or diversifying selection, has been proposed as a
107 balancing selection mechanism maintaining the diversity of *B. burgdorferi* genotypes through
108 adaptation to host 'niches' (11, 12, 18, 19). This model was applied to the maintenance of the
109 polymorphism in the outer surface protein C (OspC), one of the most diverse Lyme borreliae
110 antigens that is heavily targeted by the vertebrate immune system (20-22). Alternatively (or
111 concurrently), the OspC polymorphism could be maintained in a host-independent manner,
112 through negative frequency-dependent selection. In this form of balancing selection, rare *B.*
113 *burgdorferi OspC* genotypes to which few hosts have been exposed would have a selective
114 advantage over the more common genotypes to which many hosts have mounted an adaptive
115 immune response; thus maintaining diversity in the population (14, 17, 23-25). Theoretical studies
116 have examined patterns of OspC diversity predicted by the different proposed eco-evolutionary
117 mechanisms in different ecological settings (25-28), but a mechanistic understanding of the cellular
118 and immunological mechanisms mediating strain-host interactions is critical to disentangle the
119 multiple co-occurring selective pressures.

120 In this study, we simultaneously assessed cellular and immunological mechanisms that mediate
121 strain-host interactions using three *B. burgdorferi* strains with variable *ospC* genotypes, as well as
122 the North American rodent and avian reservoir hosts, American robins (hereafter robins) and
123 white-footed mice (*Peromyscus leucopus*), respectively. We aimed to determine which cellular
124 and immunological mechanisms mediate fitness variation in strain-host species pairs. Specifically,
125 we identified genotypic differences across *B. burgdorferi* interacting with hosts in (1) the role of
126 complement inhibition and inflammation induction; (2) the role of bacterial adhesion; (3) the role
127 of antibodies in driving late stage persistence in specific hosts and (4) transmission efficiency to
128 larval ticks. By characterizing these mechanisms, we aimed to identify plausible selective
129 pressures that shape the composition of *B. burgdorferi* strain community, its diversity, and
130 population dynamics.
131

132 **RESULTS**

133 ***Borrelia burgdorferi* B31-5A4, 297, and cN40 differed in their adhesiveness to fibroblasts, *ex***
134 ***vivo* cytokine induction, and infection establishment in robins and white-footed mice.** To
135 compare the capability of genotypically distinct *B. burgdorferi* to initiate infection in reservoir
136 hosts, the cloned *B. burgdorferi* strains B31-5A4, 297, and cN40 belonging to different genotypes
137 (Table S1) and displaying similar growth rates *in vitro* (Fig. S1) were used in this study. Bacterial
138 burdens at inoculation sites of skin and in blood were determined at 1 day after each of these strains
139 was intradermally introduced into robins and white-footed mice. We did not detect any of these
140 strains in robin blood (Fig. S2A), in agreement with no hematogenous dissemination at such an
141 early time point (29). However, we found that B31-5A4 and cN40 showed significantly higher
142 spirochete burdens at the initial injection sites, compared to mock-infected robins (Fig. 1). The

143 injection sites from only two out of four 297-inoculated robins had spirochete burdens higher than
144 detection limits (10 bacteria per 100ng of DNA from tissues), leading to non-significant
145 differences in the levels of colonization from mock-infected robins (Fig. 1A). In white-footed mice
146 infections, we did not observe spirochete burdens higher than detection limits of any of these
147 strains in the blood of white-footed mice (Fig. S2B). Nonetheless, the burdens of B31-5A4 and
148 297 were significantly higher than those from mock-infected individuals at the inoculation site
149 (~10^2 bacteria per 100ng of DNA). Only two of five white-footed mice had cN40 bacterial loads
150 greater than the detectable threshold limit, resulting in non-significant differences in burdens from
151 mock-infected mice (Fig. 1B). These findings indicate B31-5A4, 297, and cN40 have the capacity
152 to establish infection selectively in robins and white-footed mice.

153 As the burdens of *B. burgdorferi* during infection initiation can be attributed to differences in
154 spirochete attachment to cells or clearance by host inflammatory responses, we incubated B31-
155 5A4, 297, and cN40 with fibroblasts isolated from robin or white-footed mouse for 1 h and
156 determined the levels of bacterial attachment using fluorescent microscopy (Fig. S3). A non-
157 adhesive *B. burgdorferi* strain B314 was also included as control (Table S1). Compared to B314,
158 we found that B31-5A4, 297, and cN40 more efficiently bind to the fibroblasts from robins (Fig.
159 1C) or white-footed mice (Fig. 1D). Whereas B31-5A4 and cN40 bound to robin fibroblasts at
160 significantly higher levels compared to 297 (Fig. 1C), B31-5A4 and 297 attached to white-footed
161 mouse fibroblasts at significantly greater levels compared to cN40 (Fig. 1D). To determine
162 whether B31-5A4, 297, and cN40 trigger differential pro-inflammatory responses in fibroblasts
163 from different reservoir origins, we measured the expression levels of the genes encoding pro-
164 inflammatory cytokines, IFNγ and TNF, or the proteins related to these cytokines after incubating
165 cells with each of the spirochete strains for 24h. The expression levels of housekeeping genes (18S

166 rRNA and β-actin) were also included as controls. We found that the levels of expression for each
167 of the genes in any spirochete-treated cells were not significantly different from the mock-treated
168 cells at 1 to 10 of the spirochetes to cell ratio (Fig. S4). At 1 to 100 of spirochete to cell ratio, the
169 B31-5A4- or cN40-treated robin fibroblasts expressed similar levels of the tested cytokines to the
170 cells under mock treatment while 297-incubated cells had significantly greater expression of IFNγ
171 and TNF-induced protein than mock-treated cells, respectively (Fig. 1F and G). Conversely, while
172 white-footed mouse fibroblasts incubated with B31-5A4 or 297 expressed those cytokines
173 indistinguishably from mock-treated cells, cN40-treated cells showed significantly higher
174 expression of IFNγ and TNF (4.6- and 30.1-fold, respectively) than the cells under mock treatment
175 (Fig. 1I and J). These results suggest that *B. burgdorferi* B31-5A4, 297, and cN40 differ in their
176 fibroblast adhesiveness and cytokine induction in a host-dependent fashion.
177
178 **Ticks acquired different levels of *B. burgdorferi* B31-5A4, 297, and cN40 from robins and**
179 **white-footed mice infected with each of these spirochete strains.** To compare reservoir host
180 competence to B31-5A4, 297, and cN40, we assessed spirochete transmission from host to feeding
181 larvae. Unfed *I. scapularis* nymphs were allowed to feed on robins or white-footed mice until
182 repletion. We subsequently measured bacterial loads in flat and fed nymphs and found
183 indistinguishable burdens among these ticks (~10^4 bacteria per nymph), indicating no differences
184 of the ability for any tested strain to survive in flat or fed nymphs (Fig. S5).
185 We then placed *I. scapularis* larvae on robins or white-footed mice at different time points (Fig.
186 2A) to determine spirochete burdens in each larva and the percentage of spirochete-positive larvae
187 per individual host (defined as percent positivity). The spirochete burdens in uninfected (control)
188 robin-derived larvae were below the detection limit (10 bacteria per tick), resulting in zero

189 spirochete positivity at 14, 28, 35, and 56 days post nymph feeding (dpf) (Fig. 2B to F and Table
190 1). At least 18% of larvae feeding on B31-5A4-, 297-, or cN40-infected robins were spirochete
191 positive at all time points with greater than detection limits of bacterial loads, indicating the ability
192 of robins to persistently maintain and transmit these strains (Fig. 2C to F and Table 1). The percent
193 positivity of fed larvae carrying cN40 was significantly higher than those harboring 297 at all four
194 time points and significantly greater than those carrying B31-5A4 at 28, 35, and 56 dpf (Fig. 2B
195 and Table 1). Moreover, the cN40-infected larvae had significantly higher bacterial loads than the
196 297-infected larvae at all time points and significantly greater than those in B31-5A4-infected
197 larvae at 28, 35, and 56dpf (Fig. 2C to F). These data suggest that the cN40 is maintained and
198 transmitted more efficiently in robins than B31-5A4 and 297.

199 Similarly, we found bacterial burdens lower than detection limits in the larvae feeding on
200 uninfected (control) mice, resulting in zero spirochete positivity (Fig. 2G to K, Table 1). At least
201 9% of the larvae feeding on B31-5A4-, 297-, or cN40-infected mice were positive throughout the
202 experiment (Fig. 2G and Table 1). The bacterial loads from those mice were also statistically
203 different from those derived from uninfected mice (Fig. 2H to K), except that larvae infected with
204 cN40 had similar spirochete burdens to uninfected mouse-derived larvae at 56dpi. These data
205 indicate the ability of white-footed mice to maintain and transmit each of these strains. We found
206 significantly lower spirochete positivity in larvae infected with 297, compared to that in larvae
207 infected with B31-5A4 at 28 and 35 dpf, respectively ($p < 0.05$, Fig. 2G, I, J and Table 1). Finally,
208 larvae infected with cN40 showed more than significantly lower spirochete positivity (Fig. 2G and
209 Table 1) and had significantly less bacterial burdens than B31-5A4- and 297-infected ticks
210 throughout the experiments (Fig. 2H to K). These data suggest less capability of white-footed mice
211 to maintain and transmit cN40 compared to B31-5A4 or 297.

212

213 ***Borrelia burgdorferi* B31-5A4, 297, and cN40 varied in their capability to trigger bacteremia**
214 **and persistently colonize robins and white-footed mice.** We next determined the ability of B31-
215 5A4, 297, and cN40 to survive in the bloodstream of robins and white-footed mice. We found that
216 robins infected with cN40 develop significantly greater levels of bacteremia at 7, 14, and 21dpf
217 than the uninfected robins, which had spirochete burdens lower than the detection limits (10
218 bacteria per 100ng DNA, Fig. 3A to C). However, the burdens of that strain in the blood was no
219 statistically different from those in uninfected robins at 28dpf (Fig. 3D). Robins infected with 297
220 had spirochete burdens in the blood no statistically different from uninfected robins at 7, 21 and
221 28 dpf but developed statistically greater bacterial loads at 14dpf (Fig. 3A to D). Though B31-5A4
222 was capable of inducing bacteremia in robins at 7 and 14dpf at the levels statistically greater than
223 those in uninfected robins, the burdens of this strain in the blood were not statistically different
224 from those in uninfected robins at 21 and 28dpf (Fig. 3A to D). These results indicate the ability
225 of cN40 to induce long-lasting bacteremia in robins, compared to other strains, and 297 displayed
226 delayed onsets of bacteremia. Similar to uninfected robins, uninfected white-footed mice did not
227 exhibit bacteremia above the levels of detection throughout the experiment (Fig. 3E to H). At 21
228 and 28dpf, the spirochetes burdens in the blood from the mice infected with any of tested strains
229 were no statistically different from those in uninfected mice (Fig. 3E and H). At 7 and 14 dpf, B31-
230 5A4 and 297 triggered significantly higher levels of bacteremia than uninfected mice (Fig. 3E and
231 F). However, the majority of mice infected with cN40 did not show detectable bacteremia (3/5 and
232 5/5 mouse blood had burdens below detection limits at 7 and 14dpf, respectively), resulting in no
233 significant different bacterial loads from uninfected mice (Fig. 3E and F). These data suggest that

234 cN40 is less capable of surviving in the white-footed mouse bloodstream compared to B31-5A4
235 and 297, in contrast to the results derived from robins.

236 We also evaluated the ability of B31-5A4, 297, and cN40 to colonize robin and white-footed
237 mouse tissues at 64dpf (Fig. 2A). Robins infected with each of these strains had significantly
238 greater spirochete burdens in skin than uninfected robins, which exhibited bacterial loads below
239 the detection limits (Fig. 3I). In addition, spirochetes were detected at significantly greater burdens
240 in the heart and brain of cN40-infected robins and the heart of robins infected with B31-5A4,
241 compared to respective tissues from uninfected robins (Fig. 3J and K). Majority of the 297- or
242 cN40-infected robins (3 out of 4 and 3 out of 5 in 297- and cN40-infected robins, respectively)
243 had burdens below the detection limits in livers, yielding no significantly different burdens from
244 those in uninfected robins (Fig. 3L). Similarly, the burdens of B31-5A4 in the livers from
245 spirochete-infected robins were no significantly different from those from uninfected robins (Fig.
246 3L). These data showed persistent skin colonization of strains B31-5A4, 297, and cN40 in robin,
247 but the ability of each strain to colonize other tissues varied (Fig. 3I to L). We also measured the
248 bacterial burdens at 64dpf in the tissues from white-footed mice infected with each of these strains.
249 We detected spirochetes in ears, tibiofemoral joints, heart, and bladder from mice infected with
250 B31-5A4 or 297 (~10^2 to 10^3 bacteria per 100ng of DNA from tissues). The bacterial burdens in
251 tibiofemoral joints, heart, and bladder from B31-5A4- or 297- but not cN40-infected mice were
252 significantly greater than those in uninfected mice (Fig. 3M to P). These findings demonstrated
253 the ability of B31-5A4 and 297 but not cN40 to persistently colonize white-footed mice.

254

255 **Robin but not white-footed mouse complement differentiated the ability of *B. burgdorferi***
256 **B31-5A4, 297, and cN40 to survive in sera.** To define the capability of B31-5A4, 297, and cN40

257 to evade complement-mediated killing, we evaluated the percent survival after incubation of these
258 strains individually with the sera from uninfected robins or white-footed mice by counting the
259 number of motile bacteria under microscopes. More than 95% of all tested strains including a
260 serum sensitive control strain, *B. burgdorferi* B313 (30), survived in heat inactivated robin sera,
261 in which the heat sensitive components such as complement were not functional (Fig. 4A and
262 Table S1). Less than 16% of B313 remained motile, verifying the bactericidal activity of these
263 robin sera (Fig. 4A). More than 85% of B31-5A4 and cN40 were alive, but only 50% of 297 was
264 motile after incubated with robin sera (Fig. 4A). However, all strains survived at similar levels
265 (greater than 80% of live spirochetes) in the sera pre-treated with OmCI, which inactivates robin
266 complement by abolishing the lytic activity towards gram negative bacteria (Fig. 4B) (31). These
267 results indicate that the 297 is more vulnerable to robin complement-mediated killing than B31-
268 5A4 and cN40. We also determined the ability of spirochete strains to evade killing by white-
269 footed mouse complement in the similar fashion. Greater than 95% of B313, B31-5A4, 297, and
270 cN40 survived in heat inactivated white-footed mouse sera (Fig. 4C). Whereas only 29% of B313
271 remained motile after treated with these sera, more than 97% of other tested strains were alive in
272 the untreated white-footed mouse sera (Fig. 4C). More than 93% of tested strains remained motile
273 in white-footed mouse sera treated with CVF, which inactivates mammal complement (Fig. 4D)
274 (32). These results indicate that all tested strains evade the killing by white-footed mouse
275 complement at indistinguishable levels.
276
277 **Robins and white-footed mice generated different levels of pro-inflammatory cytokines in**
278 **response to early infection of *B. burgdorferi* B31-5A4, 297, and cN40.** We compared the levels
279 of pro-inflammatory cytokines, IFNγ and TNFα, in the sera derived from robin- and white-footed

280 mice at different times during the infection. We found no significant different levels of IFNγ and
281 TNFα in robins prior to the infection among different infection groups (Fig. 5A and E). At 7dpf,
282 B31-5A4- or cN40-infected robins were not significantly different in those cytokines compared to
283 uninfected robins, 297-infected robins produced significantly greater levels of IFNγ and TNFα
284 than those uninfected birds, respectively (Fig. 5B and F). At 14dpf, the levels of these cytokines
285 from those robins are no different from those in uninfected robins. In contrast to robins at 7dpf,
286 cN40-infected mice displayed significantly higher levels of these cytokines than uninfected mice
287 at this time point while 297-infected mice had no significantly different in the levels of those
288 cytokines, compared to uninfected mice (Fig. 5J and N). Note that B31-5A4-infected mice had
289 significantly greater levels of IFNγ (Fig. 5J) but were not significantly different from levels of
290 TNFα at 7dpf (Fig. 5N), compared to uninfected mice. These data indicate differences of pro-
291 inflammatory cytokine induction by each of these spirochete strains, particularly at early stages of
292 robin and white-footed mouse infection.
293
294 **Robins and white-footed mice developed distinct levels of bactericidal antibodies during**
295 **early infection of *B. burgdorferi* B31-5A4, 297, or cN40.** We aimed to quantitatively measure
296 the levels of antibodies induced by the infection of B31-5A4, 297, and cN40. To avoid the
297 confounding factors of strain-specific antibody recognition observed previously (10, 33), we
298 mixed these strains and determined the IgG titers against such mixtures in robins infected with
299 B31-5A4, 297, or cN40. We found that robins infected with any strain develop significantly higher
300 anti-spirochete IgG titers than uninfected robins at 14, 21, and 28dpf whereas only 297-infected
301 robins had significantly higher tiers of IgG than uninfected robins at 7dpf (Fig. 6B to E). cN40
302 triggered significantly greater levels of IgG antibodies compared to the other strains at 21 and 28

dpf whereas 297 induced IgG titers significantly higher than those titers triggered by other strains at 7dpf (Fig. 6B, D and E). Further, we found that white-footed mice infected with each of these strains had anti-spirochete IgG titers at more robust levels than uninfected mice at 14, 21, and 28dpf whereas only cN40-infected mice developed significantly higher tiers of IgG than uninfected white-footed mice at 7dpf (Fig. 6G to J). cN40 induced significantly lower titers of such IgG at 21 and 28dpf but significantly higher titers at 7dpf, compared to B31-5A4 and 297 (Fig. 6G, I and J). These results indicate that B31-5A4, 297, and cN40 differ in their ability to induce antibodies, and such differences depend on the hosts and infection onset.

The levels of antibodies against B31-5A4, 297, or cN40 at 7dpf in robins and white-footed mice negatively corresponded to the ability of these hosts to carry spirochetes (Fig. 2B and G). This finding raised a hypothesis that such correspondences are mediated by bactericidal activities of those antibodies. We thus tested this hypothesis by incubating a mixture of B31-5A4, 297, and cN40 with different dilution rates of sera from robins or white-footed mice infected with each of these strains at 7dpf. We found that B31-5A4- and cN40-derived robin sera did not kill spirochetes at any of the tested dilution rates, similar to sera from uninfected robins. However, 297-derived sera eliminated 50% of spirochetes at the dilution rate of 1:52× (Fig. 6K). Conversely, B31-5A4- and 297-derived white-footed mouse sera did not eliminate spirochetes, similar to the sera from uninfected mice. However, cN40-derived sera eliminated 50% of spirochetes at the dilution rate of 1:32× (Fig. 6L). These finding showed different levels of bactericidal activities from the antibodies produced by B31-5A4-, 297-, or cN40-infected robins and white-footed mice early during infection.

DISCUSSION

326 Theory predicts that generalist vectors should select for generalist pathogens, to minimize the
327 latter's loss to incompetent hosts. Host-specialized genospecies in *B. burgdorferi* s.l. thus represent
328 a paradox, with the intriguing possibility of incipient host specialization within genotypes of the
329 generalist *B. burgdorferi*. We present evidence of molecular mechanisms that differentially
330 influence the ability of three strains of *B. burgdorferi* to colonize, disseminate to distal tissues,
331 evade host immune responses, and be transmitted from the host to feeding ticks between two
332 representative natural reservoir hosts (Fig. 7). We found that cellular and immunological
333 mechanisms act mostly synergistically, resulting in increased fitness of strain cN40 in robins and
334 297 in white-footed mice. Contrary to theoretical expectations, strain B31-5A4 was able to
335 efficiently infect both hosts, with higher fitness in white-footed mice than the 'specialized' strain,
336 297, and exhibited intermediate fitness in robins. The synergistic nature of those cellular and
337 immunological mechanisms indicates a strong selective pressure for the evolution of host
338 specialization, as predicted by the MNP theory. However, the higher overall fitness of B31-5A4
339 does not support the existence of tradeoffs, with this strain having high fitness in both
340 representative hosts. This higher fitness advantage is consistent with the high overall prevalence
341 of the genotype of this strain (RST type 1/OspC type A) circulating in Lyme disease prevalent
342 regions of North America (10, 13, 34-37).

343 Multiple mechanisms were tested in this study for their role in contributing to host specialization
344 of *B. burgdorferi*. At one day after intradermal infection of spirochetes, we found that *B.*
345 *burgdorferi* B31-5A4 and cN40 colonized robin inoculation sites (skin tissue) more efficiently
346 than 297, whereas B31-5A4 and 297 colonized the inoculation sites of white-footed mice at
347 significantly higher levels than cN40. We also found that these strains differed in their capability
348 to attach to robin and white-footed mouse skin fibroblasts *in vitro*. These results showed that strain-

349 to-strain variability of fibroblast adhesion is host-dependent and corresponds to the ability of *B.*
350 *burgdorferi* spirochetes to colonize the inoculation sites of these hosts immediately after infection.
351 This supports prior findings of Lyme borreliae strains varying in their adhesive activities (38),
352 demonstrating the role of such cellular processes (adhesion) in conferring strain-host associations.
353 However, the levels of robin fibroblast adhesion of B31-5A4, 297, and cN40 did not perfectly
354 agree to strain colonization of other tissues (e.g. brain and liver) in robins at 64 days after being
355 fed on by *B. burgdorferi*-infected nymphs. Additionally, strain 297 colonized robin skin at similar
356 levels to B31 and cN40 at 64 dpf, but this strain attached to robin fibroblast at lower levels than
357 other strains. These disagreements between fibroblast adhesion/early colonization of inoculation
358 sites and tissue colonization at later stages suggest the possibility of adhesion-independent
359 mechanisms to determine strain-host associations. In fact, the complement system is the first line
360 of immune defense in vertebrate animal sera and confers Lyme borreliae clearance as soon as
361 infection begins (39, 40). Our findings of greater percentages of B31-5A4 and cN40 surviving in
362 robin sera, compared to those of 297, mirror the trends of these spirochete strains being maintained
363 at earlier infection onsets (e.g. 14 dpf) and early bloodstream survival of *B. burgdorferi* (e.g. 7
364 dpf). These results imply that the host complement plays a role in determining spirochete
365 genotype-specific robin competence. In contrast, all three *B. burgdorferi* strains showed similar
366 levels of survival in the presence of white-footed mouse sera, suggesting a non-complement-
367 mediated defense mechanism to dominate the association of white-footed mice with these
368 spirochetes.
369 In addition to complement, we compared the cytokine production in responding to the presence
370 of genotypically distinct *B. burgdorferi*. Cytokines are generally triggered shortly after pathogen
371 invasions, often leading to activation of different pathways and downstream bactericidal responses

372 as a bottleneck of infection initiation (i.e. recruitment of innate and adaptive immune cells) (41-
373 45). *Borrelia burgdorferi* strain-to-strain variability in inducing pro-inflammatory cytokines has
374 been observed in humans, *Mus musculus*, and *P. leucopus* mice or from cells derived from these
375 animals (46-52). In humans, the levels of multiple cytokines are positively correlated with disease
376 severity but are independent from spirochete burdens (46, 47, 53-55). We found that the three
377 tested *B. burgdorferi* strains differed in their ability, in robins and white-footed mouse fibroblasts,
378 to induce the expression of two pro-inflammatory cytokines and their related proteins, IFNγ, TNFα,
379 and TNFα-induced proteins. Such differences also matched the variation of these strains to trigger
380 IFNγ and TNFα during early infection. The ability of these strains to induce those pro-
381 inflammatory cytokines were negatively associated with larval percent positivity from the
382 infection of these *B. burgdorferi* strains. These results raised the hypothesis that less robust host
383 cytokine induction by spirochetes facilitates reservoir competence, and differences in cytokine
384 induction by genotypically distinct spirochetes shape Lyme borreliae-reservoir associations.

385 Following the induction of innate immune responses, the adaptive responses including
386 antibodies are essential in Lyme borreliae clearance by vertebrates (41, 56, 57). Distinct levels of
387 antibodies were observed during the infection time period by different spirochete strains (10, 58).
388 We observed at 7 dpf that 297 and cN40 triggered significantly higher titers of anti-*B. burgdorferi*
389 IgG in robins and white-footed mice, respectively, compared to the other spirochete strains.
390 Furthermore, *B. burgdorferi* was selectively eliminated by the sera collected at 7dpf from robins
391 infected with 297 or white-footed mice infected with cN40, suggesting that the antibody response
392 varies among different spirochete strain-host pairings. Interestingly, a previous study showed
393 variable IgG levels against lp36- and lp28-1-derived proteins in white-footed mice infected with
394 different *B. burgdorferi* strains (10). However, in that study, those lp36- and lp28-1-derived

395 proteins were produced from a single strain of *B. burgdorferi* (*B. burgdorferi* strain B31), leading
396 to the possibility that allelic-specific recognition is the result of antigenic sequence variation
397 among spirochete strains (10, 33, 59-61). Thus, the possibility of the antibodies against other
398 spirochete proteins to confer *B. burgdorferi* clearance may not be completely ruled out. Our
399 finding of early antibody-mediated bactericidal activities in robin and white-footed mouse sera
400 highlights the potential role of antibodies in dictating pathogen-host associations. We observed
401 high titers of antibody responses at late time points (21 and 28 dpf) in robins infected with cN40
402 and mice infected with B31-5A4- or 297. Nonetheless, cN40 was persistently maintained in robins
403 whereas B31-5A4 and 297 efficiently survived long-term in white-footed mice. Such observations
404 are consistent with the evidence of pathogen-specific antibodies present in persistently infected
405 animals (62-64). These results thus suggest inefficient spirochete elimination by those antibodies
406 at later stages of infection. That inefficient pathogen killing could be because of the onset-
407 dependent reduction of highly antigenic spirochete proteins (i.e. downregulation of OspC at late
408 infection onsets) (65-69), constantly changing features of antigen sequences to evade antibody
409 responses (i.e. VlsE) (70-72), or the rapid dissemination of spirochetes to the sites less vulnerable
410 to antibody-mediated clearance (73).

411 Our results suggest spirochete adhesiveness and early immune responses as the cellular and
412 immunological mechanisms that differentially confer spirochete fitness in reservoir-strain-host
413 combinations (Fig. 7). Both mechanisms could play in concert to determine *B. burgdorferi* strain-
414 to-strain variation in host fitness. Our findings support previous studies which determined that
415 some polymorphic Lyme borreliae proteins confer these immune response functions in a variant-
416 specific manner, and such manner is host dependent (30, 59, 62, 63, 74-80). The potential for host
417 specialization driving genome-wide diversification is illustrated by the recent definition of a new

418 species of *B. burgdorferi* s.l., *B. bavariensis*, which was previously considered a genotype of the
419 avian associated species, *B. garinii*. Such a redefinition is based on the variation in chromosomal
420 housekeeping genes and the association of this species with rodents, unlike other *B. garinii* strains
421 (81). This reclassification reflects how host adaptation can lead to speciation in Lyme borreliae
422 (82). Prior field studies along with our current laboratory evidence showing incipient host
423 specialization raises the possibility of diversification of *B. burgdorferi* in North America into
424 multiple genospecies. Here, we used a controlled laboratory setup to demonstrate differences in
425 fitness of *B. burgdorferi* strains in North American reservoir hosts. The molecular mechanisms
426 supported by our findings provide a potential model of how specific adaptations may lead to
427 specialization even with a significant cost in lost propagules to incompetent hosts. The identified
428 mechanisms can guide future empirical and modeling studies to understand the role of host-
429 pathogen-vector interactions in shaping the microparasite host ranges and their potential for
430 pathogen spillover into livestock, wildlife or humans.
431

432 **MATERIALS AND METHODS**

433 **Ethics statement.** All experiments involving American robins (*Turdus migratorius*) and white-
434 footed mice (*Peromyscus leucopus*) were performed in strict accordance with all provisions of the
435 Animal Welfare Act, the Guide for the Care and Use of Laboratory Animals, and the PHS Policy
436 on Humane Care and Use of Laboratory Animals. Additionally, the protocol was approved by the
437 Institutional Animal Care and Use Committee (IACUC) of Wadsworth Center, New York State
438 Department of Health (Protocol docket number 18-412 and 19-451), and Columbia University
439 (Protocol number AC-AAAY2450), and the City University in New York Advanced Science
440 Research Center (Protocol number ASRC AUP 2016-20). To mistnet robins, personnel were

441 approved on scientific collecting permits USFWS Collecting Permit MB035731 and NYSDEC
442 Permit #1236.
443
444 **Bird, Mouse, Tick, and Bacterial strains.** From June-July, 2019 and July, 2020, American robins
445 were mist netted around the property of Griffin Laboratory of Wadsworth Center, New York State
446 Department of Health at Albany, NY. This site was selected because of previously reported low
447 tick abundance, thus minimizing the probability of previous tick exposure. Sera were collected
448 from 32 and 17 robins in 2019 and 2020, respectively, using BD Microtainer Capillary Blood
449 Collector tubes (Fisher Scientific, Hampton, NH, USA) to assess previous infection with *B.*
450 *burgdorferi* infection by the methods previously described (31). To confirm seronegative status,
451 robins were quarantined for two weeks at 25°C on a 12L:12D (light: dark) cycle by housing them
452 in cages with a wire bottom, under which a water moat was placed. If replete ticks were found
453 while the birds were in quarantine, quantitative PCR (qPCR) was used to determine the spirochete
454 burdens in those ticks (see "Quantification of *B. burgdorferi* in infected ticks, tissues, and blood
455 samples" for more details). The birds with spirochete positive ticks attached were removed from
456 the experiments. After two weeks of quarantine, robins were subjected to additional serological
457 examination as described above, and 40 seronegative juvenile (hatch year) robins were considered
458 non-infectious and used in this study.
459 White-footed mice were purchased from the *Peromyscus* Genetic Stock Center at the University
460 of South Carolina (Columbia, SC). Non-sibling mice were bred in-house at Columbia University.
461 Immunodeficient Fox Chase SCID mice (C.B.17 SCID) were obtained from Charles River (Boston,
462 MA) and used to generate infected nymphs for each *B. burgdorferi* strain as described in the
463 "Mouse infection experiments by ticks" section. *Ixodes scapularis* larvae were purchased from the

464 National Tick Research and Education Center, Oklahoma State University (Stillwater, OK). Mice
465 and birds were housed individually and maintained at 21 to 24°C on a 14L:10D (light: dark) cycle
466 and handled humanely. The *B. burgdorferi* strains used in this study were cultivated in BSK-II
467 completed medium as described in Table 1 (83).
468
469 **Determination of spirochete growth curves and generation time.** *Borrelia burgdorferi* strains
470 B31-5A4, 297, and cN40 were cultivated in BSK-II complete media at 33°C in the initial
471 concentration of 5×10^6 ml^{-1}. The concentration of spirochetes was measured prior to incubation
472 and at 24-, 48-, 72-, 96-, 120-, 144-, and 168-h post incubation using a Nikon Eclipse E600 dark
473 field microscope (Nikon, Melville, NY). The generation time of each spirochete strain at the
474 exponential phase was calculated as described previously (84).
475
476 **Robin, C.B.17 SCID mouse, and white-footed mouse infection by intradermal inoculation.**
477 Four to eight week old male or female white-footed mice, American robins, or C.B.17 SCID mice
478 were intradermally inoculated, using a 27-gauge needle, with *B. burgdorferi* B31-5A4, 297, cN40,
479 or BSK-II medium without rabbit sera (1×10^5 bacteria per C.B.17 SCID mouse or 1×10^4 bacteria
480 per robin or white-footed mouse) as a control (63). The plasmid profiles and the presence of the
481 shuttle plasmids of each of these *B. burgdorferi* strains were verified prior to infection to ensure
482 no loss of plasmids, as described previously (85-87). Both robins and white-footed mice were
483 euthanized at one day post injection. The inoculation site of the skin and blood from robins and
484 white-footed mice were collected to quantitatively evaluate spirochete burdens as described in the
485 "Quantification of *B. burgdorferi* in infected ticks, tissues and blood samples" section.
486

487 **Quantification of *B. burgdorferi* in infected ticks, tissues, and blood samples.** The white-footed
488 mouse- or robin-derived replete nymphs were mixed with glass beads and homogenized by a
489 Precellys 24 High-Powered Bead Mill Homogenizer (Bertin, Rockville, MD). DNA was extracted
490 from blood and tissue samples of white-footed mice, robins and homogenized ticks using an EZ-
491 10 Genomic DNA kit (Biobasic, Amherst, NY). The quantity and quality of DNA for each tissue
492 sample was assessed by measuring the concentration of DNA and the ratio of the UV absorption
493 at 280 to 260 using a nanodrop 1000 UV/Vis spectrophotometer (ThermoFisher Scientific,
494 Waltham, MA). The amount of DNA used in this study was 100 ng for each sample, and the
495 280:260 ratio was between 1.75 to 1.85, indicating the lack of contamination by RNA or proteins.
496 qPCR was performed to quantitate bacterial loads. *Borrelia burgdorferi* genomic equivalents were
497 calculated using an Applied Biosystems 7500 Real-Time PCR system (ThermoFisher Scientific)
498 in conjunction with PowerUp SYBR Green Master Mix (ThermoFisher Scientific), based on
499 amplification of the *B. burgdorferi 16S rRNA* gene using primers 16S rRNAfp and 16S rRNArp
500 (Table S2), as described previously (88). Cycling parameters for SYBR green-based reactions
501 were 50°C for 2 min, 95°C for 10 min, 45 cycles of 95°C for 15 s, and 60°C for 1 min. The number
502 of *16S rRNA* copies was calculated by establishing a threshold cycle (Ct) standard curve of a
503 known number of *16S rRNA* gene copies extracted from *B. burgdorferi* strain B31, and compared
504 to the Ct values of the experimental samples. To ensure low signals were not simply a function of
505 the presence of PCR inhibitors in the DNA preparation, five samples of blood, tibiofemoral joints,
506 bladders of white-footed mice and the skin, brain, and heart of robins in the B31-5A4 experimental
507 group were applied to qPCR to determine the levels of β-actin from white-footed mice (pActfp
508 and pActrp) and robins (rActfp and rActrp), respectively (Table S2) (63, 89). Note that the primers
509 used to determine the expression of the genes encoding robin actin were based on the mRNA

510 sequences that were translated to protein (Genbank Accession number: PYHW01009720.1) from
511 a closely related avian host, rufous-bellied thrush (*Turdus rufiventris*) due to the lack of sequence
512 information of American robin actin. As predicted, we detected 10^7 copies of the actin gene from
513 100ng of each DNA sample in robins and white-footed mice, ruling out the presence of PCR
514 inhibitors in these samples.
515
516 **Isolation of robin fibroblasts.** The procedures to isolate robin fibroblasts were described
517 previously (90). Five 5mm × 5mm sections of skin were removed from the breast of euthanized
518 robins, washed twice in PBS buffer, and then incubated in a transferring solution until the next
519 step was ready to be performed. The constituents of the transferring solution included Dulbecco's
520 modified Eagle medium (DMEM) (Wadsworth media & tissue culture core) with glucose (4.5mg
521 ml^{-1}) (Sigma-Aldrich, St. Louis, MO), sodium pyruvate (110mg l^{-1}) (Sigma-Aldrich), L-glutamine
522 (ThermoFisher Scientific), supplemented with 10% heat-inactivated fetal bovine serum
523 (ThermoFisher Scientific), 2% heat-inactivated chicken serum (Biowest, Riverside, MO, USA),
524 and antibiotics (100U ml^{-1} of mixture of penicillin and streptomycin) (ThermoFisher Scientific).
525 The skin was then submerged in 70% ethanol (Sigma-Aldrich) for 30s, minced using sterile
526 scalpels, and placed in collagenase B at 37°C overnight (ThermoFisher Scientific). We then
527 applied the mixture of the cells to a 20µm cell strainer and spun down the samples. The pellets
528 containing fibroblasts were re-suspended in growth media and incubated at 37°C with 5% CO_2.
529 Growth media had the same components as the transferring solution except it was supplemented
530 with amphotericin B (ThermoFisher Scientific) to a concentration of 0.25µg/ml. The cells were
531 harvested by trypsinization using Trypsin (0.25% trypsin in DMEM media, ThermoFisher
532 Scientific) and used in the spirochete attachment experiment.

533

534 **Determination of the levels of spirochete attachment to robin and white-footed mouse**
535 **fibroblasts.** The primary fibroblasts from the neck skin of American robins (see the previous
536 section) and ears of white-footed mice were acquired commercially (#AG22353, Coriell Institute
537 for Medical Research, Camden, NJ) and cultivated on cover slips in 24-well plates (2×10^5 cells
538 per well). *Borrelia burgdorferi* strains B31-5A4, 297, cN40, or B314 were suspended in BSK-II
539 medium and added to prepared plates (2×10^6 spirochetes per well). The plates were centrifuged
540 at 106 g for 5 min and then rocked at room temperature for 1 h. After removing unbound bacteria
541 through washing each well with PBS containing 0.2% BSA, the bound bacteria and cells on the
542 cover slips were fixed using 100% chilled methanol for 1 h followed by blocking with PBS
543 containing 0.2% BSA for 1 h. After washing with PBS containing 0.2% BSA, the cover slips were
544 incubated with a fluorescein isothiocyanate (FITC)-conjugated goat anti-*B. burgdorferi* polyclonal
545 antibody (Abcam, Cambridge, MA) for 1 h and mounted using ProLong Gold antifade mountant
546 with DAPI fluorescent stain (ThermoFisher Scientific). The spirochetes (green) and the DNA from
547 spirochetes and the nuclei of fibroblasts (blue) were then visualized under overlaid FITC and DAPI
548 filters using an Olympus BX51 fluorescence microscope (Olympus Corporation, Waltham, MA)
549 (Fig. S3). The number of spirochetes from three fields of view were counted in four independent
550 events. The results were presented as the average number of spirochetes per 50 fibroblast cells.

551

552 **Determination of the relative expression levels of the genes encoding IFNγ and TNFα or**
553 **TNFα-induced proteins in fibroblasts by quantitative reverse transcription PCR (RT-qPCR).**
554 The procedures for the examination of expression levels in the genes encoding cytokines of
555 fibroblasts were described previously (52). In brief, the primary fibroblasts from robins and white-

556 footed mice were cultivated in 24-well plates (2×10^5 cell per well). When the cells were greater
557 than 80% confluent, *B. burgdorferi* strains B31-5A4, 297, or cN40 suspended in BSK-II medium
558 were added to corresponding wells on each plate (2×10^6 and 2×10^7 spirochetes per well for the
559 cell to spirochete ratio (MOI) of 1:10 and 1:100, respectively) for 24h. The cells incubated with
560 BSK-II medium without bacteria (mock-treated cells) were included as a control.

561 After incubation, the supernatant was removed, and the cells were washed with PBS buffer.
562 These fibroblasts were then suspended in Trizol (ThermoFisher Scientific) at room temperature
563 for 1 h to inactivate RNase. The procedure of RNA extraction was performed using Direct-Zol
564 RNA MiniPrep Plus Kit (Zymo Research, Irvine, CA) as previously described (84), and DNA was
565 removed using RQ1 RNase-Free DNase (Promega, Madison, WI). We then synthesized cDNA
566 using these RNA samples (1 μg per sample) by qScript cDNA SuperMix (Quanta Bioscience,
567 Beverly, MA). The expression levels of the house keeping genes encoding the 18S rRNA gene
568 from robins (Genbank Accession number: M59402.1) or white-footed mice (Genbank Accession
569 number: AY591913.1) were included as controls. The primers used to quantitate the expression of
570 the genes encoding white-footed mouse IFNγ, TNF, and 18S rRNA, and robin IFNγ, TNFα-
571 induced proteins, and 18S rRNA are listed in Table S2 (89). Note, because of the lack of sequence
572 information for robin cytokines, the primers to determine the expression of these cytokines were
573 based on the mRNA sequences of IFNγ (Genbank Accession number: PYHW01010552.1) and
574 TNFα-induced proteins (Genbank Accession number: PYHW01009717.1) from rufous-bellied
575 thrush (*Turdus rufiventris*). The quantity and quality of cDNA for each sample was evaluated by
576 obtaining the concentration of DNA and the ratio of the UV absorption at 260 and 280 using a
577 Nanodrop 1000 UV/Vis spectrophotometer (ThermoFisher, Waltham, MA). The resulting ratio
578 between 1.75 and 1.85, indicated the lack of RNA or protein contamination. Samples were applied

579 to an Applied Biosystems 7500 Real-Time PCR System (ThermoFisher) in conjunction with
580 PowerUp SYBR Green Master Mix (ThermoFisher) to detect the expression levels of the above-
581 mentioned genes. The cycling parameters were 50°C for 2 min, 95°C for 10 min, and 45 cycles of
582 95°C for 15 s, and 49°C for 1 min, and the resulting values of threshold cycles (Ct) were
583 determined from duplicate experiments in three independent events. The relative expression of the
584 genes encoding IFNγ, TNF, TNFα-induced proteins, or 18S rRNA was presented by normalizing
585 the Ct-derived from each of these cytokines to that of β-actin from respective animals through the
586 following equation (Equation 1).

587 $$\textit{cytokine expression relative to actin} = 2^{-(Ct(cytokines)-Ct(actin))} \quad \text{(Equation 1)}$$

588

589 **Generation of *B. burgdorferi*-infected nymphal ticks.** Four-week-old male and female C.B.17
590 SCID mice were injected with a concentration of $1x10^5$ of either *B. burgdorferi* strain B31-5A4,
591 297, or cN40 via subcutaneous injection. The plasmid profiles and the presence of the shuttle
592 vector of each of these *B. burgdorferi* strains were verified prior to injection to ensure no loss of
593 plasmids, as previously described (85-87). SCID mice inoculated with BSK-II media without
594 rabbit sera were used to generate uninfected nymphs. A 3 mm ear biopsy was collected 7 days post
595 injection from each mouse inoculated with a *B. burgdorferi* strain and DNA was extracted using a
596 DNeasy Blood and Tissue kit (Qiagen, Germantown, MD). DNA from ear tissue was subjected to
597 qPCR analysis to verify infection in each host (30). At 14 days post injection, approximately 200
598 larvae were placed in the ears of anesthetized mice using a paint brush. Mice were anesthetized
599 with isoflurane for 45 min to allow larvae to attach before being housed individually in water bath
600 cages, larvae were allowed to feed to repletion, as described previously (30, 91). Engorged larvae
601 were collected, cleaned with 10% bleach and 70% ethanol solutions, and stored in an incubator at

602 21°C, 95% relative humidity, and a 14L:10D light: dark cycle. Larvae molted into the nymphal
603 life stage in approximately 4-6 weeks and were used in the subsequent experiments with white-
604 footed mice and robins.
605
606 **Robin and white-footed mouse infection by nymphs.** The timeline of experimental procedures
607 is provided in Fig. 2A. Basically, unfed nymphs carrying B31-5A4, 297, cN40 or unfed, uninfected
608 nymphs were placed in the ear canals of each mouse (*n* = 5 mice per group, 5 nymphs in each ear).
609 Mice were maintained under anesthesia for 60 min to allow nymphs to attach before being placed
610 individually in water bath cages. Approximately 100 to 150 xenodiagnostic larvae were placed on
611 each mouse at 14, 28, 35, and 56 days post nymph feeding using the aforementioned procedure.
612 To permit flat nymphs to feed on robins, the birds were placed into a PVC pipe (~2.5-3.0 inches
613 in diameter; 10 inches in length) as described (92). After unfed nymphs carrying B31-5A4, 297,
614 cN40 or unfed, uninfected nymphs were placed on these robins (*n* = 5 robins per group, 10 nymphs
615 per bird), the PVC pipes were covered by a fine mosquito net ('no-see-um' netting, Skeeta,
616 Bradenton, FL) secured with a rubber band. The birds were then moved into wire bottom cages
617 with a water moat. These tick-infested robins were kept in a dark room for 1 h to minimize
618 grooming and allow ticks to attach before they were released and returned to their cages. To allow
619 xenodiagnostic larvae to feed on robins, approximately 100 to 200 naïve larvae were placed on
620 robins restrained in the PVC pipes as described above at 14, 28, 35, and 56 days post nymph
621 feeding.
622 Blood samples were collected from each animal (robins and white-footed mice) prior to nymph
623 feeding and at 7, 14, 21, and 28 days post nymph feeding. The skin, heart, liver, and brain from
624 robins and the ears, tibiofemoral joints, heart, and bladder from white-footed mice were obtained

625 at 64 days post nymphs feeding. The blood, tissues, and replete nymphs collected from each animal
626 were analyzed via qPCR to determine spirochete burdens as described in the section
627 "Quantification of *B. burgdorferi* in infected ticks, tissues, and blood samples".
628
629 **Serum resistance assays.** Serum resistance of *B. burgdorferi* strains was determined as described
630 previously with modifications (30, 84). The mid-log phase of *B. burgdorferi* strains B31-5A4, 297,
631 and cN40 as well as a high passage, serum sensitive strain B313 (negative control) were cultivated
632 in triplicate. The resulting spirochete culture was diluted to a final concentration of 5×10^6 bacteria
633 per milliliter into BSK-II medium without rabbit sera. The cell suspensions were mixed with sera
634 collected from naïve white-footed mice or robins (60% spirochetes and 40% sera) in the presence
635 or absence of 2 μM of cobra venom factor (CVF) or recombinant *Ornithordorus moubata*
636 complement inhibitor (OmCI). The generation of recombinant OmCI has been described
637 previously (31). The sera were incubated at 65°C for 2 h (heat-inactivated sera) and included as a
638 control. At 0 and 4 h following incubation with sera, the number of motile spirochetes was
639 measured under dark field microscopy. The percent survival of *B. burgdorferi* was calculated by
640 the normalization of motile spirochetes at 4 h post incubation to that immediately after incubation
641 with sera.
642
643 **Determination of the relative levels of IFNγ and TNFα in sera by ELISA.** Due to the lack of
644 commercially available ELISA kits to detect robin cytokines, the kits for chicken IFNγ
645 (ThermoFisher) and TNFα (Genorise, Glen Mills, PA) were used to measure the levels of those
646 cytokines in robins based on the absorption values derived from ELISA. Similarly, the ELISA kits
647 to determine the levels of IFNγ and TNFα from house mouse (*Mus muscuslus*) (Tonbo Bioscience,

648 San Diego, CA) were utilized to detect those cytokines in white-footed mice. We observed the
649 antibodies in the ELISA kits cross reacted with IFNγ and TNFα from robins and white-footed mice.
650 However, the recombinant proteins provided in these kits to generate standard curves were based
651 on the sequences from chicken and house mouse IFNγ and TNFα, potentially leading to inaccuracy
652 of quantification for those cytokines by normalizing the results obtained from robin and white-
653 footed mouse samples to standard curves. Therefore, we chose to present reservoir animal
654 cytokines as relative levels (arbitrary unit; A.U.), similar to a previous study (93). In brief, the
655 monoclonal capture antibodies that recognized chicken or house mouse IFNγ or TNFα were coated
656 on microtiter plate wells. After blocked by 5% PBS-BSA, different dilutions (1:100×, 1:300×, or
657 1:900×) of sera from robins and white-footed mice at 0, 7, 14, or 21 days post nymph feeding were
658 added to the wells. Wells were washed using PBST buffer (PBS with 0.5% of Tween 20) and the
659 detection of antibodies against chicken or house mouse IFNγ or TNFα were incubated for 1 h at
660 room temperature. The wells were then washed with PBST buffer and subsequently mixed with a
661 tetramethyl benzidine solution (ThermoFisher). The absorbance level was detected at 620nm for
662 10 cycles of 60 s kinetic intervals with 10 s of shaking duration in a Sunrise absorbance ELISA
663 plate reader (Tecan, Männedorf, Switzerland). We then obtained the greatest maximum slope of
664 optical density/min per sample multiplied by respective serum dilution factors to represent the
665 relative levels of cytokines shown as arbitrary units.
666
667 **Determination of the titers of the antibodies against spirochetes.** The titers of IgG against
668 spirochetes were measured as described previously with modifications (94). Basically, microtiter
669 plate wells were coated with a mixture of *B. burgdorferi* B31, 297, and cN40 (1×10^6 spirochetes
670 per strain in a well). After blocking with 5% PBS-BSA, the sera from white-footed mice or robins

671 collected at 7, 14, 21, 28, and 56 days post nymph feeding were diluted in 50µl of PBS (1:100×,
672 1:300×, or 1:900×) and then added to the wells. After the samples were washed with PBST buffer,
673 the microtiter wells were incubated with antibodies that recognize the Fc region of IgG from *P.*
674 *leucopus* (1:1,000×, Serocare, Inc, Milford, MA), or wild bird (1:10,000×, Bethyl laboratory,
675 Montgomery, TX). After the addition of these antibodies, tetramethyl benzidine solution
676 (ThermoFisher) was added, and the absorbance was detected at 620nm for 10 cycles of 60 s kinetic
677 intervals with 10 s of shaking duration in a Sunrise absorbance ELISA plate reader (Tecan,
678 Männedorf, Switzerland). The values of greatest maximum slopes of optical density/min/sample
679 were multiplied by respective serum dilution factors as shown as arbitrary units, representing
680 antibody titers.
681
682 **Borreliacidal assays.** Sera collected from robins and white-footed mice at 7 days post tick feeding
683 were used to measure the bactericidal activity against *B. burgdorferi* as described previously (95).
684 The complement in these serum samples was heat-inactivated by incubating these samples at 55°C
685 for 2 h. The heat inactivated sera were serially diluted in BSK-II media without rabbit sera
686 followed by being mixed with complement-preserved sera from guinea pig (Sigma-Aldrich) or
687 chicken (Biowest, Riverside). Heat-inactivated guinea pig and chicken sera were included as
688 controls. *Borrelia burgdorferi* strains B31-5A4, 297, or cN40 (1×10^7 spirochetes per strain) were
689 then mixed prior to their addition to the reaction. At 24 h after incubation, the surviving spirochetes
690 were quantified by counting the motile bacteria under dark-field microscopy and presented as the
691 proportion of serum-treated to untreated spirochetes. We also calculated the 50% borreliacidal titer
692 (BA), which represents the serum dilution rate that eradicates 50% of spirochetes, using dose-
693 response stimulation fitting in GraphPad Prism 7.

Statistical analyses. Because the data were not normally distributed, we used a Kruskal-Wallis test followed by a two-stage step-up method with a Benjamini, Krieger, and Yekutieli correction for all comparisons (96). Geometric means of duplicated individual samples (qPCR) were used in our calculations. Spirochete burdens among the three *B. burgdorferi* strains (B31-5A4, 297, and cN40) and uninfected samples in robins, white-footed mice, or ticks were compared using normalized qPCR quantity values for each individual. Cell adhesion variation among the *B. burgdorferi* strains were analyzed using the number of spirochetes per 50 fibroblast cells observed under fluorescent microscopy while the variation in expression levels of the genes encoding IFN-γ, TNF, or TNFα-induced protein were first normalized by the gene encoding actin and then significant differences between the constitutively expressed gene, actin, and 18S rRNA were determined using RT-qPCR quantity values. However, when comparing the differences between levels of pro-inflammatory cytokines at early stages of host infection, we used quantitative ELISA values. Spirochete survival in treated and untreated host sera was assessed using the number of mobile spirochetes at 4 h post incubation. We used quantitative ELISA values to determine the significant differences among the *B. burgdorferi* strains and levels of IgG antibody production in robins and white-footed mice. All analyses and figure generation were completed using GraphPad Prism 7 software.

ACKNOWLEDGEMENTS

We thank Thomas Hart and Tristan Nowak for graph editing, and Jen Owen and Jean Tsao for technical support in the protocol of tick infection in robins. We also thank Thomas Hart, Patricia Lederman, Tristan Nowak, and Frank Blaisdell for the husbandry work to maintain tick colony

and robins. We are grateful for John Leong and George Chaconas for sharing the *B. burgdorferi* strains B31-5A4, 297, and cN40, Sudha Chaturvedi allowing us to use her Bead Homogenizer, Susan Madison-Antenucci allowing us to use her fluorescence microscope, and Noel Espina for the assistance with that microscope. We thank Wadsworth Media & Tissue Culture Core for preparation of *Borrelia* and American robin and white-footed mouse fibroblast culture medium. This work was supported by NSF IOS-1755370 (DMT, MC and MDW), NSF-IOS1755286 (YL, ADII, ALM, JS, and LDK), New York State Department of Health Wadsworth Center Start-Up Grant (ALM and YL). The funders had no role in study design, data collection and analysis, decision to publish, or preparation of the manuscript. The authors declare that the research was conducted in the absence of any commercial or financial relationships that could be construed as a potential conflict of interest.

REFERENCES

1. Poulin R. KBR, Morand S. Micromammals and Macroparasites. Tokyo: Springer; 2006. 233-56 p.

2. Futuyma DJ, Moreno, G. The evolution of ecological specialization. Ann Rev Ecol Syst 1988;19:207-33.

3. Tufts DM, Hart TM, Chen GF, Kolokotronis SO, Diuk-Wasser MA, Lin YP. Outer surface protein polymorphisms linked to host-spirochete association in Lyme borreliae. Molecular microbiology. 2019.

4. Lin YP, Diuk-Wasser MA, Stevenson B, Kraiczy P. Complement Evasion Contributes to Lyme Borreliae-Host Associations. Trends in parasitology. 2020;36(7):634-45.

5. O'Keeffe KR, Oppler ZJ, Brisson D. Evolutionary ecology of Lyme *Borrelia*. Infection, genetics and evolution : journal of molecular epidemiology and evolutionary genetics in infectious diseases. 2020:104570.

6. Kurtenbach K, De Michelis S, Etti S, Schafer SM, Sewell HS, Brade V, et al. Host association of *Borrelia burgdorferi* sensu lato--the key role of host complement. Trends in microbiology. 2002;10(2):74-9.

7. Kurtenbach K, Peacey M, Rijpkema SG, Hoodless AN, Nuttall PA, Randolph SE. Differential transmission of the genospecies of *Borrelia burgdorferi* sensu lato by game birds and small rodents in England. Applied and environmental microbiology. 1998;64(4):1169-74.

8. Kurtenbach K, Schafer SM, Sewell HS, Peacey M, Hoodless A, Nuttall PA, et al. Differential survival of Lyme borreliosis spirochetes in ticks that feed on birds. Infection and immunity. 2002;70(10):5893-5.

9. Hanincova K, Ogden NH, Diuk-Wasser M, Pappas CJ, Iyer R, Fish D, et al. Fitness variation of *Borrelia burgdorferi* sensu stricto strains in mice. Applied and environmental microbiology. 2008;74(1):153-7.

10. Baum E, Hue F, Barbour AG. Experimental infections of the reservoir species *Peromyscus leucopus* with diverse strains of Borrelia burgdorferi, a Lyme disease agent. mBio. 2012;3(6):e00434-12.

11. Hanincova K, Kurtenbach K, Diuk-Wasser M, Brei B, Fish D. Epidemic spread of Lyme borreliosis, northeastern United States. Emerging infectious diseases. 2006;12(4):604-11.

12. Brisson D, Dykhuizen DE. ospC diversity in *Borrelia burgdorferi*: different hosts are different niches. Genetics. 2004;168(2):713-22.

13. Vuong HB, Canham CD, Fonseca DM, Brisson D, Morin PJ, Smouse PE, et al. Occurrence and transmission efficiencies of *Borrelia burgdorferi ospC* types in avian and mammalian wildlife. Infection, genetics and evolution : journal of molecular epidemiology and evolutionary genetics in infectious diseases. 2014;27:594-600.

14. Kurtenbach K, Hanincova K, Tsao JI, Margos G, Fish D, Ogden NH. Fundamental processes in the evolutionary ecology of Lyme borreliosis. Nature reviews Microbiology. 2006;4(9):660-9.

15. Haven J, Magori K, Park AW. Ecological and inhost factors promoting distinct parasite life-history strategies in Lyme borreliosis. Epidemics. 2012;4(3):152-7.

16. Qiu WG, Bosler EM, Campbell JR, Ugine GD, Wang IN, Luft BJ, et al. A population genetic study of *Borrelia burgdorferi* sensu stricto from eastern Long Island, New York, suggested frequency-dependent selection, gene flow and host adaptation. Hereditas. 1997;127(3):203-16.

17. Qiu WG, Dykhuizen DE, Acosta MS, Luft BJ. Geographic uniformity of the Lyme disease spirochete (*Borrelia burgdorferi*) and its shared history with tick vector (*Ixodes scapularis*) in the Northeastern United States. Genetics. 2002;160(3):833-49.

18. Brisson D, Dykhuizen DE, Ostfeld RS. Conspicuous impacts of inconspicuous hosts on the Lyme disease epidemic. Proc Biol Sci. 2008;275(1631):227-35.

19. Brisson D, Baxamusa N, Schwartz I, Wormser GP. Biodiversity of *Borrelia burgdorferi* strains in tissues of Lyme disease patients. PloS one. 2011;6(8):e22926.

20. Xu Q, Seemanapalli SV, McShan K, Liang FT. Constitutive expression of outer surface protein C diminishes the ability of *Borrelia burgdorferi* to evade specific humoral immunity. Infection and immunity. 2006;74(9):5177-84.

21. Tilly K, Krum JG, Bestor A, Jewett MW, Grimm D, Bueschel D, et al. *Borrelia burgdorferi* OspC protein required exclusively in a crucial early stage of mammalian infection. Infection and immunity. 2006;74(6):3554-64.

22. Liang FT, Yan J, Mbow ML, Sviat SL, Gilmore RD, Mamula M, et al. *Borrelia burgdorferi* changes its surface antigenic expression in response to host immune responses. Infection and immunity. 2004;72(10):5759-67.

23. Andersson M, Scherman K, Raberg L. Multiple-strain infections of *Borrelia afzelii*: a role for within-host interactions in the maintenance of antigenic diversity? Am Nat. 2013;181(4):545-54.

24. Brisson D, Dykhuizen DE. A modest model explains the distribution and abundance of *Borrelia burgdorferi* strains. The American journal of tropical medicine and hygiene. 2006;74(4):615-22.

25. Haven J, Vargas LC, Mongodin EF, Xue V, Hernandez Y, Pagan P, et al. Pervasive recombination and sympatric genome diversification driven by frequency-dependent selection in *Borrelia burgdorfer*i, the Lyme disease bacterium. Genetics. 2011;189(3):951-66.

26. Woolhouse ME, Taylor LH, Haydon DT. Population biology of multihost pathogens. Science. 2001;292(5519):1109-12.

27. Gog JR, Grenfell BT. Dynamics and selection of many-strain pathogens. Proceedings of the National Academy of Sciences of the United States of America. 2002;99(26):17209-14.

28. Barrett LG, Thrall PH, Burdon JJ, Linde CC. Life history determines genetic structure and evolutionary potential of host-parasite interactions. Trends Ecol Evol. 2008;23(12):678-85.

29. Barthold SW, Persing DH, Armstrong AL, Peeples RA. Kinetics of *Borrelia burgdorferi* dissemination and evolution of disease after intradermal inoculation of mice. The American journal of pathology. 1991;139(2):263-73.

30. Hart T, Nguyen NTT, Nowak NA, Zhang F, Linhardt RJ, Diuk-Wasser M, et al. Polymorphic factor H-binding activity of CspA protects Lyme borreliae from the host complement in feeding ticks to facilitate tick-to-host transmission. PLoS pathogens. 2018;14(5):e1007106.

31. Frye AM, Hart TM, Tufts DM, Ram S, Diuk-Wasser MA, Kraiczy P, et al. A soft tick *Ornithodoros moubata* salivary protein OmCI is a potent inhibitor to prevent avian complement activation. Ticks and tick-borne diseases. 2020;11(2):101354.

32. Finnie JA, Stewart RB, Aston WP. A comparison of cobra venom factor-induced depletion of serum C3 in eight different strains of mice. Dev Comp Immunol. 1981;5(4):697-701.

33. Ivanova L, Christova I, Neves V, Aroso M, Meirelles L, Brisson D, et al. Comprehensive seroprofiling of sixteen *B. burgdorferi* OspC: implications for Lyme disease diagnostics design. Clinical immunology. 2009;132(3):393-400.

34. States SL, Brinkerhoff RJ, Carpi G, Steeves TK, Folsom-O'Keefe C, DeVeaux M, et al. Lyme disease risk not amplified in a species-poor vertebrate community: similar *Borrelia burgdorferi* tick infection prevalence and OspC genotype frequencies. Infection, genetics and evolution : journal of molecular epidemiology and evolutionary genetics in infectious diseases. 2014;27:566-75.

35. Wormser GP, Brisson D, Liveris D, Hanincova K, Sandigursky S, Nowakowski J, et al. *Borrelia burgdorferi* genotype predicts the capacity for hematogenous dissemination during early Lyme disease. The Journal of infectious diseases. 2008;198(9):1358-64.

36. Jones KL, Glickstein LJ, Damle N, Sikand VK, McHugh G, Steere AC. *Borrelia burgdorferi* genetic markers and disseminated disease in patients with early Lyme disease. Journal of clinical microbiology. 2006;44(12):4407-13.

37. Wang G, Ojaimi C, Wu H, Saksenberg V, Iyer R, Liveris D, et al. Disease severity in a murine model of lyme borreliosis is associated with the genotype of the infecting *Borrelia burgdorferi* sensu stricto strain. The Journal of infectious diseases. 2002;186(6):782-91.

38. Parveen N, Robbins D, Leong JM. Strain variation in glycosaminoglycan recognition influences cell-type-specific binding by lyme disease spirochetes. Infection and immunity. 1999;67(4):1743-9.

39. Zipfel PF, Skerka C. Complement regulators and inhibitory proteins. Nature reviews Immunology. 2009;9(10):729-40.

40. Sjoberg AP, Trouw LA, Blom AM. Complement activation and inhibition: a delicate balance. Trends in immunology. 2009;30(2):83-90.

41. Tracy KE, Baumgarth N. Borrelia burgdorferi Manipulates Innate and Adaptive Immunity to Establish Persistence in Rodent Reservoir Hosts. Frontiers in immunology. 2017;8:116.

42. Hyde JA. Borrelia burgdorferi Keeps Moving and Carries on: A Review of Borrelial Dissemination and Invasion. Frontiers in immunology. 2017;8:114.

43. Liu N, Montgomery RR, Barthold SW, Bockenstedt LK. Myeloid differentiation antigen 88 deficiency impairs pathogen clearance but does not alter inflammation in *Borrelia burgdorferi*-infected mice. Infection and immunity. 2004;72(6):3195-203.

44. Bolz DD, Sundsbak RS, Ma Y, Akira S, Kirschning CJ, Zachary JF, et al. MyD88 plays a unique role in host defense but not arthritis development in Lyme disease. Journal of immunology. 2004;173(3):2003-10.

45. Troy EB, Lin T, Gao L, Lazinski DW, Camilli A, Norris SJ, et al. Understanding barriers to *Borrelia burgdorferi* dissemination during infection using massively parallel sequencing. Infection and immunity. 2013;81(7):2347-57.

46. Strle K, Jones KL, Drouin EE, Li X, Steere AC. *Borrelia burgdorferi* RST1 (OspC type A) genotype is associated with greater inflammation and more severe Lyme disease. The American journal of pathology. 2011;178(6):2726-39.

47. Cerar T, Strle F, Stupica D, Ruzic-Sabljic E, McHugh G, Steere AC, et al. Differences in Genotype, Clinical Features, and Inflammatory Potential of *Borrelia burgdorferi* sensu stricto Strains from Europe and the United States. Emerging infectious diseases. 2016;22(5):818-27.

48. Petzke MM, Iyer R, Love AC, Spieler Z, Brooks A, Schwartz I. *Borrelia burgdorferi* induces a type I interferon response during early stages of disseminated infection in mice. BMC microbiology. 2016;16:29.

49. Mason LM, Herkes EA, Krupna-Gaylord MA, Oei A, van der Poll T, Wormser GP, et al. *Borrelia burgdorferi* clinical isolates induce human innate immune responses that are not dependent on genotype. Immunobiology. 2015;220(10):1141-50.

50. Wang G, Petzke MM, Iyer R, Wu H, Schwartz I. Pattern of proinflammatory cytokine induction in RAW264.7 mouse macrophages is identical for virulent and attenuated *Borrelia burgdorferi*. Journal of immunology. 2008;180(12):8306-15.

51. Kern A, Schnell G, Bernard Q, Boeuf A, Jaulhac B, Collin E, et al. Heterogeneity of *Borrelia burgdorferi* Sensu Stricto Population and Its Involvement in *Borrelia* Pathogenicity: Study on Murine Model with Specific Emphasis on the Skin Interface. PloS one. 2015;10(7):e0133195.

52. Schramm F, Kern A, Barthel C, Nadaud S, Meyer N, Jaulhac B, et al. Microarray analyses of inflammation response of human dermal fibroblasts to different strains of *Borrelia burgdorferi* sensu stricto. PloS one. 2012;7(6):e40046.

53. Li X, McHugh GA, Damle N, Sikand VK, Glickstein L, Steere AC. Burden and viability of *Borrelia burgdorferi* in skin and joints of patients with erythema migrans or lyme arthritis. Arthritis and rheumatism. 2011;63(8):2238-47.

54. Jones KL, McHugh GA, Glickstein LJ, Steere AC. Analysis of *Borrelia burgdorferi* genotypes in patients with Lyme arthritis: High frequency of ribosomal RNA intergenic spacer type 1 strains in antibiotic-refractory arthritis. Arthritis and rheumatism. 2009;60(7):2174-82.

55. Dykhuizen DE, Brisson D, Sandigursky S, Wormser GP, Nowakowski J, Nadelman RB, et al. The propensity of different *Borrelia burgdorferi* sensu stricto genotypes to cause disseminated infections in humans. The American journal of tropical medicine and hygiene. 2008;78(5):806-10.

56. Barthold SW, Bockenstedt LK. Passive immunizing activity of sera from mice infected with *Borrelia burgdorferi*. Infection and immunity. 1993;61(11):4696-702.

57. Fikrig E, Bockenstedt LK, Barthold SW, Chen M, Tao H, Ali-Salaam P, et al. Sera from patients with chronic Lyme disease protect mice from Lyme borreliosis. The Journal of infectious diseases. 1994;169(3):568-74.

58. Wang G, Ojaimi C, Iyer R, Saksenberg V, McClain SA, Wormser GP, et al. Impact of genotypic variation of *Borrelia burgdorferi* sensu stricto on kinetics of dissemination and severity of disease in C3H/HeJ mice. Infection and immunity. 2001;69(7):4303-12.

59. Benoit VM, Fischer JR, Lin YP, Parveen N, Leong JM. Allelic variation of the Lyme disease spirochete adhesin DbpA influences spirochetal binding to decorin, dermatan sulfate, and mammalian cells. Infection and immunity. 2011;79(9):3501-9.

60. Roberts WC, Mullikin BA, Lathigra R, Hanson MS. Molecular analysis of sequence heterogeneity among genes encoding decorin binding proteins A and B of *Borrelia burgdorferi* sensu lato. Infection and immunity. 1998;66(11):5275-85.

61. Wilske B, Preac-Mursic V, Jauris S, Hofmann A, Pradel I, Soutschek E, et al. Immunological and molecular polymorphisms of OspC, an immunodominant major outer surface protein of Borrelia burgdorferi. Infection and immunity. 1993;61(5):2182-91.

62. Lin YP, Tan X, Caine JA, Castellanos M, Chaconas G, Coburn J, et al. Strain-specific joint invasion and colonization by Lyme disease spirochetes is promoted by outer surface protein C. PLoS pathogens. 2020;16(5):e1008516.

63. Lin YP, Benoit V, Yang X, Martinez-Herranz R, Pal U, Leong JM. Strain-specific variation of the decorin-binding adhesin DbpA influences the tissue tropism of the lyme disease spirochete. PLoS pathogens. 2014;10(7):e1004238.

64. Isogai E, Tanaka S, Braga IS, 3rd, Itakura C, Isogai H, Kimura K, et al. Experimental *Borrelia garinii* infection of Japanese quail. Infection and immunity. 1994;62(8):3580-2.

65. Schwan TG, Piesman J, Golde WT, Dolan MC, Rosa PA. Induction of an outer surface protein on *Borrelia burgdorferi* during tick feeding. Proceedings of the National Academy of Sciences of the United States of America. 1995;92(7):2909-13.

66. Hodzic E, Feng S, Freet KJ, Borjesson DL, Barthold SW. *Borrelia burgdorferi* population kinetics and selected gene expression at the host-vector interface. Infection and immunity. 2002;70(7):3382-8.

67. Hodzic E, Feng S, Freet KJ, Barthold SW. *Borrelia burgdorferi* population dynamics and prototype gene expression during infection of immunocompetent and immunodeficient mice. Infection and immunity. 2003;71(9):5042-55.

68. Bykowski T, Woodman ME, Cooley AE, Brissette CA, Brade V, Wallich R, et al. Coordinated expression of *Borrelia burgdorferi* complement regulator-acquiring surface proteins during the Lyme disease spirochete's mammal-tick infection cycle. Infection and immunity. 2007;75(9):4227-36.

69. Iyer R, Caimano MJ, Luthra A, Axline D, Jr., Corona A, Iacobas DA, et al. Stage-specific global alterations in the transcriptomes of Lyme disease spirochetes during tick feeding and following mammalian host adaptation. Molecular microbiology. 2015;95(3):509-38.

70. Zhang JR, Hardham JM, Barbour AG, Norris SJ. Antigenic variation in Lyme disease borreliae by promiscuous recombination of VMP-like sequence cassettes. Cell. 1997;89(2):275-85.

71. Verhey TB, Castellanos M, Chaconas G. Analysis of recombinational switching at the antigenic variation locus of the Lyme spirochete using a novel PacBio sequencing pipeline. Molecular microbiology. 2018;107(1):104-15.

72. Coutte L, Botkin DJ, Gao L, Norris SJ. Detailed analysis of sequence changes occurring during *vlsE* antigenic variation in the mouse model of *Borrelia burgdorferi* infection. PLoS pathogens. 2009;5(2):e1000293.

73. Shih CM, Telford SR, 3rd, Pollack RJ, Spielman A. Rapid dissemination by the agent of Lyme disease in hosts that permit fulminating infection. Infection and immunity. 1993;61(6):2396-9.

74. Caine JA, Lin YP, Kessler JR, Sato H, Leong JM, Coburn J. *Borrelia burgdorferi* outer surface protein C (OspC) binds complement component C4b and confers bloodstream survival. Cellular microbiology. 2017.

75. Lagal V, Portnoi D, Faure G, Postic D, Baranton G. *Borrelia burgdorferi* sensu stricto invasiveness is correlated with OspC-plasminogen affinity. Microbes and infection / Institut Pasteur. 2006;8(3):645-52.

76. Rogers EA, Marconi RT. Delineation of species-specific binding properties of the CspZ protein (BBH06) of Lyme disease spirochetes: evidence for new contributions to the pathogenesis of *Borrelia* spp. Infection and immunity. 2007;75(11):5272-81.

77. Wallich R, Pattathu J, Kitiratschky V, Brenner C, Zipfel PF, Brade V, et al. Identification and functional characterization of complement regulator-acquiring surface protein 1 of the Lyme disease spirochetes *Borrelia afzelii* and *Borrelia garinii*. Infection and immunity. 2005;73(4):2351-9.

78. Hammerschmidt C, Koenigs A, Siegel C, Hallstrom T, Skerka C, Wallich R, et al. Versatile roles of CspA orthologs in complement inactivation of serum-resistant Lyme disease spirochetes. Infection and immunity. 2014;82(1):380-92.

79. Alitalo A, Meri T, Comstedt P, Jeffery L, Tornberg J, Strandin T, et al. Expression of complement factor H binding immunoevasion proteins in *Borrelia garinii* isolated from patients with neuroborreliosis. European journal of immunology. 2005;35(10):3043-53.

80. Xie J, Zhi H, Garrigues RJ, Keightley A, Garcia BL, Skare JT. Structural determination of the complement inhibitory domain of *Borrelia burgdorferi* BBK32 provides insight into classical pathway complement evasion by Lyme disease spirochetes. PLoS pathogens. 2019;15(3):e1007659.

81. Margos G, Vollmer SA, Cornet M, Garnier M, Fingerle V, Wilske B, et al. A new *Borrelia* species defined by multilocus sequence analysis of housekeeping genes. Applied and environmental microbiology. 2009;75(16):5410-6.

82. Norte AC, Margos G, Becker NS, Albino Ramos J, Nuncio MS, Fingerle V, et al. Host dispersal shapes the population structure of a tick-borne bacterial pathogen. Mol Ecol. 2019.

83. Barbour AG. Isolation and cultivation of Lyme disease spirochetes. The Yale journal of biology and medicine. 1984;57(4):521-5.

84. Marcinkiewicz AL, Dupuis AP, 2nd, Zamba-Campero M, Nowak N, Kraiczy P, Ram S, et al. Blood treatment of Lyme borreliae demonstrates the mechanism of CspZ-mediated complement evasion to promote systemic infection in vertebrate hosts. Cellular microbiology. 2019;21(2):e12998.

85. Purser JE, Norris SJ. Correlation between plasmid content and infectivity in *Borrelia burgdorferi*. Proceedings of the National Academy of Sciences of the United States of America. 2000;97(25):13865-70.

86. Blevins JS, Hagman KE, Norgard MV. Assessment of decorin-binding protein A to the infectivity of *Borrelia burgdorferi* in the murine models of needle and tick infection. BMC microbiology. 2008;8:82.

87. Chan K, Casjens S, Parveen N. Detection of established virulence genes and plasmids to differentiate *Borrelia burgdorferi* strains. Infection and immunity. 2012;80(4):1519-29.

88. Marcinkiewicz AL, Lieknina I, Yang X, Lederman PL, Hart TM, Yates J, et al. The Factor H-Binding Site of CspZ as a Protective Target against Multistrain, Tick-Transmitted Lyme Disease. Infection and immunity. 2020;88(5).

89. Izuogu AO, McNally KL, Harris SE, Youseff BH, Presloid JB, Burlak C, et al. Interferon signaling in *Peromyscus leucopus* confers a potent and specific restriction to vector-borne flaviviruses. PloS one. 2017;12(6):e0179781.

90. Calhoon EA, Miller, M. K., Jimenez, A. G., Harper, J. M., Williams, J. B. . Changes in cultured dermal fibroblasts during early passages across five wild bird species. Canadian Journal of Zoology. 2013;91:653-9.

91. Kern A, Zhou CW, Jia F, Xu Q, Hu LT. Live-vaccinia virus encapsulation in pH-sensitive polymer increases safety of a reservoir-targeted Lyme disease vaccine by targeting gastrointestinal release. Vaccine. 2016;34(38):4507-13.

92. Johnston E, Tsao JI, Munoz JD, Owen J. *Anaplasma phagocytophilum* infection in American robins and gray catbirds: an assessment of reservoir competence and disease in captive wildlife. Journal of medical entomology. 2013;50(1):163-70.

93. Varkey R, Du Q, Karnell JL, Xiao X, Casey KA, Woods R, et al. Discovery and characterization of potent IL-21 neutralizing antibodies via a novel alternating antigen immunization and humanization strategy. PloS one. 2019;14(1):e0211236.

94. Lin YP, Yu Y, Marcinkiewicz AL, Lederman P, Hart TM, Zhang F, et al. Non-anticoagulant Heparin as a Pre-exposure Prophylaxis Prevents Lyme Disease Infection. ACS Infect Dis. 2020;6(3):503-14.

95. Marcinkiewicz AL, Lieknina I, Kotelovica S, Yang X, Kraiczy P, Pal U, et al. Eliminating Factor H-Binding Activity of Borrelia burgdorferi CspZ Combined with Virus-Like Particle Conjugation Enhances Its Efficacy as a Lyme Disease Vaccine. Frontiers in immunology. 2018;9:181.

96. Benjamini YK, A. M. Yekutieli, D. . Adaptive linear step-up procedures that control the false discovery rate. Biometrika. 2006;93:491-507.

97. Burgdorfer W, Barbour AG, Hayes SF, Benach JL, Grunwaldt E, Davis JP. Lyme disease-a tick-borne spirochetosis? Science. 1982;216(4552):1317-9.

98. Leong JM, Moitoso de Vargas L, Isberg RR. Binding of cultured mammalian cells to immobilized bacteria. Infection and immunity. 1992;60(2):683-6.

99. Steere AC, Grodzicki RL, Kornblatt AN, Craft JE, Barbour AG, Burgdorfer W, et al. The spirochetal etiology of Lyme disease. The New England journal of medicine. 1983;308(13):733-40.

100. Barthold SW, de Souza MS, Janotka JL, Smith AL, Persing DH. Chronic Lyme borreliosis in the laboratory mouse. The American journal of pathology. 1993;143(3):959-71.

101. Barthold SW, Beck DS, Hansen GM, Terwilliger GA, Moody KD. Lyme borreliosis in selected strains and ages of laboratory mice. The Journal of infectious diseases. 1990;162(1):133-8.

102. Sadziene A, Wilske B, Ferdows MS, Barbour AG. The cryptic *ospC* gene of *Borrelia burgdorferi* B31 is located on a circular plasmid. Infection and immunity. 1993;61(5):2192-5.

103. Lin T, Oliver JH, Jr., Gao L. Genetic diversity of the outer surface protein C gene of southern *Borrelia* isolates and its possible epidemiological, clinical, and pathogenetic implications. Journal of clinical microbiology. 2002;40(7):2572-83.

104. Wang IN, Dykhuizen DE, Qiu W, Dunn JJ, Bosler EM, Luft BJ. Genetic diversity of *ospC* in a local population of *Borrelia burgdorferi* sensu stricto. Genetics. 1999;151(1):15-30.

105. Chan K, Awan M, Barthold SW, Parveen N. Comparative molecular analyses of *Borrelia burgdorferi* sensu stricto strains B31 and N40D10/E9 and determination of their pathogenicity. BMC microbiology. 2012;12:157.

106. Barbour AG, Travinsky B. Evolution and distribution of the ospC Gene, a transferable serotype determinant of *Borrelia burgdorferi*. mBio. 2010;1(4).

1048 **TABLES**

1049 **Table 1. The number of positive xenodiagnostic larval ticks collected from robins and white-**

1050 **footed mice.**

dpf[a]	Positive xenodiagnostic larval ticks acquired from			
	Mice fed on by naïve nymphs	Mice fed on by nymphs carrying *B. burgdorferi*		
		B31-5A4	297	cN40
American robins				
14	0/44	39/44[b]	19/44[b,c]	41/55[b]
28	0/44	18/33[b,c]	11/44[b,c]	46/55[b]
35	0/44	11/33[b,c]	12/44[b,c]	34/55[b]
56	0/44	8/33[b,c]	7/44[b,c]	30/55[b]
White-footed mice				
14	0/55	47/55[b,c]	47/55[b,c]	16/55[b]
28	0/33	50/55[b,c]	40/55[b,c]	8/55[b]
35	0/33	51/55[b,c]	40/55[b,c]	9/55[b]
56	0/33	38/55[b,c]	35/55[b,c]	5/55[b]

1051 [a]Days post nymph feeding.
1052 [b]Difference compared with larvae from the mice fed on by naïve nymphs by two-tailed Fisher test.
1053 [c]Difference compared with larvae from the mice fed on by nymphs carrying strain cN40 by two-
1054 tailed Fisher test.
1055

1056

1057

1058

1059

1060

1061

1062

1063

1064

1065

1066

1067 **FIGURE LEGENDS**

1068 **Figure 1. *Borrelia burgdorferi* B31-5A4, 297, and cN40 differed in early colonization in robins**
1069 **and white-footed mice and adhesion and cytokine triggering in these animals-derived**
1070 **fibroblasts. (A and B): (A)** American robins and **(B)** white-footed (WF) mice were intradermally
1071 inoculated with 10^4 *B. burgdorferi* B31-5A4, 297, or cN40, or with BSK-II medium without rabbit
1072 sera as mock infection ("Mock"). The inoculation site of skin from these robins and mice were
1073 collected at 1-day post infection (1dpi) to determine bacterial burdens by qPCR. The bacterial
1074 loads in the tissues or blood from robins or mice were normalized to 100 ng total DNA. Shown
1075 are the geometric mean ± geometric standard deviation of bacterial burdens in those tissues from
1076 four robins or mice per group. Significant differences ($P < 0.05$) in the spirochete burdens
1077 (normalized qPCR quantity values) relative to the mock infected group are indicated (''*''). **(C**
1078 **and D):** *B. burgdorferi* B31-5A4, 297, cN40, or B314 (negative control) (2×10^6 spirochetes) were
1079 incubated with fibroblasts (2×10^5 cells) from **(C)** American robins and **(D)** white-footed (WF)
1080 mice for 1 h. We mixed those cells with FITC-conjugated goat anti-*B. burgdorferi* polyclonal
1081 antibodies and visualized the spirochetes after fixation. Additionally, DAPI was incubated with
1082 these cells to localize the nuclei from fibroblasts. The levels of spirochete attachment were
1083 evaluated by counting the number of bacteria per 50 cells under fluorescence microscopy described
1084 in the section "Materials and Methods." Each bar represents the mean of four independent
1085 determinations ± standard deviation. Asterisks indicate significant differences ($P < 0.05$) in
1086 spirochetal attachment relative using normalized qPCR quantity values to strain B314. **(E to J):**
1087 Fibroblasts (2×10^5 cells) from **(E to G)** American robins and **(H to J)** white-footed (WF) mice
1088 were incubated for 24h with *B. burgdorferi* B31-5A4, 297, or cN40 (2×10^7 of spirochetes for
1089 spirochete to cell ration (MOI) at 1:100). Cell media-treated fibroblasts were included as control

1090 ("Mock"). After the RNA was extracted from these cells, the expression levels of the genes
1091 encoding IFN-γ, TNF, or TNFα-induced protein and the constitutively expressed gene, actin, and
1092 18S rRNA, from robins and white-footed mice were determined using quantitative reverse
1093 transcription polymerase chain reaction. The expression levels of the genes encoding **(E and H)**
1094 18S rRNA, **(F and I)** IFNγ, **(G)** TNFα-induced protein, and **(J)** TNF are presented by normalizing
1095 to the expression levels of the gene encoding actin. Each bar represents the mean of three
1096 independent determinations ± SD. The asterisk ("*") indicates significant differences ($P < 0.05$;)
1097 in the normalized expression levels of the gene encoding IFN-γ ,TNF, and TNFα-induced protein
1098 in fibroblasts treated with indicated spirochete strains relative to those in mock-treated cells.
1099

1100 **Figure 2. *Borrelia burgdorferi* B31-5A4, 297, and cN40 displayed strain-to-strain variation of**
1101 **xenodiagnostics acquisition from robins and white-footed mice. (A)** The experimental timeline
1102 of infection. **(B to K):** *Ixodes scapularis* nymphs carrying *B. burgdorferi* B31-5A4, 297, or cN40,
1103 or naïve nymphs (Uninfect.) were allowed to feed to repletion on **(B to F)** 3, 4, 5, or 4 American
1104 robins, respectively, or **(G to K)** 5 white-footed (WF) mice per group. Approximately 100 larval
1105 ticks were placed on each robin at the time points indicated in Fig. 2A to feed till repletion. qPCR
1106 was used to determine spirochete burdens derived from 55 larvae feeding on *B. burgdorferi*-
1107 infected white-footed mice or 33, 44, 55, and 44 larvae feeding on robins fed on by nymphs
1108 carrying B31-5A4, 297, or cN40, or uninfected nymphs, respectively. **(B and F)** The larvae were
1109 considered xenodiagnostic positive if their spirochete burdens were greater than the threshold, the
1110 mean plus three-fold standard deviation of spirochete burdens in the uninfected group. Shown are
1111 the means ± SEM of percent positive larvae. **(C to F and H to K)** Shown are the geometric means
1112 ± geometric standard deviation of bacterial burdens in larvae that are allowed to feed on robins or

1113 white-footed (WF) mice at **(C and H)** 14, **(D and I)** 28, **(E and J)** 35, and **(F and K)** 56 days post
1114 nymph feeding (dpf). Significant differences ($p < 0.05$) in the spirochete burdens relative to larvae
1115 feeding on naïve robins or white-footed mice (‘‘*’’) or between different groups (“#”) are
1116 indicated.
1117

1118 **Figure 3. *Borrelia burgdorferi* B31-5A4, 297, and cN40 differed in their ability to induce**
1119 **bacteremia and colonize tissues in robins and white-footed mice.** *Ixodes scapularis* nymphs
1120 carrying *B. burgdorferi* B31-5A4, 297, or cN40, or naïve nymphs (Uninfect.) were allowed to feed
1121 to repletion on **(A to D and I to L)** 3, 4, 5, and 4 American robins, respectively, or **(E to H and**
1122 **M to P)** 5 white-footed (WF) mice per group. The bacterial loads in the blood at **(A and E)** 7, **(B**
1123 **and F)** 14, **(C and G)** 21, and **(D and H)** 28 days post nymph feeding (dpf) and in **(I)** skin, **(J)**
1124 heart, **(K)** brain, and **(L)** liver of robins and **(M)** ears, **(N)** tibiofemoral joints (Tibio.), **(O)** heart,
1125 **(P)** bladder of white-footed mice at 64 days post nymph feeding (dpf) were determined by qPCR.
1126 The bacterial loads in blood were normalized to 100 ng total DNA. Shown are the geometric mean
1127 ± geometric standard deviation of indicated number of robins or white-footed mice. Significant
1128 differences ($p < 0.05$) in the spirochete burdens relative to robins or white-footed mice fed on by
1129 naïve nymphs (‘‘*’’) are indicated.
1130

1131 **Figure 4. *Borrelia burgdorferi* B31-5A4, 297, and cN40 varied in their ability to survive in**
1132 **robin but not white-footed mouse sera.** A high passage, non-infectious, serum sensitive *B.*
1133 *burgdorferi* strain B313 (“B313”) or *B. burgdorferi* B31-5A4, 297, or cN40 were incubated for 4
1134 h with the sera from American robins at a final concentration of 40% in the **(A)** absence or **(B)**
1135 presence of 2 μM of OmCI. Each of these spirochete strains was also incubated for 4 h with the

1136 sera from white-footed (WF) mice at a final concentration of 40% in the **(C)** absence or **(D)**
1137 presence of 2 μM of CVF. The above-mentioned sera were also heat-inactivated and included as
1138 controls. The number of motile spirochetes was assessed microscopically. The percentage of
1139 survival for *B. burgdorferi* was calculated using the number of mobile spirochetes at 4 h post
1140 incubation normalized to that prior to the incubation with serum. The assays were performed at
1141 three independent occasions; within each experiment, samples were run in triplicate, and the
1142 survival percentage for each experiment was calculated by averaging the results from triplicate
1143 runs. The result shown here are the average ± standard deviation of the survival percentage from
1144 three independent experiments. Significant differences ($P < 0.05$) of the percent survival of
1145 spirochetes between groups are indicated (#).
1146
1147 **Figure 5. *Borrelia burgdorferi* B31-5A4, 297, and cN40 triggered different levels of pro-**
1148 **inflammatory cytokines at early stages of robin and white-footed mice infection.** *Ixodes*
1149 *scapularis* nymphs infected with *B. burgdorferi* B31-5A4, 297, cN40, or naïve nymphs (Uninfect.)
1150 were allowed to feed to repletion on **(A to H)** American robins or **(I to P)** white-footed (WF) mice.
1151 The sera were obtained **(A, E, I, and M)** prior to tick feeding or at **(B, F, J, and N)** 7-, (**C, G, K,**
1152 **and O)** 14-, or **(D, H, L, and P)** 21-days post nymph feeding ("dpf"). The levels of IFNγ **(A to D**
1153 **and I to L)** and TNFα **(E to H and M to P)** were determined using quantitative ELISA. Shown
1154 are the geometric mean ± geometric standard deviation of five white-footed mice per group or
1155 robins (3, 4, 5, and 4 for the strains B31-5A4-, 297-, cN40-infected robins or uninfected robins per
1156 group, respectively). Significant differences ($p < 0.05$) in the cytokine levels relative to robins or
1157 white-footed mice fed on by naïve nymphs (''*'') are indicated.
1158

1159 **Figure 6. *Borrelia burgdorferi* B31-5A4, 297, and cN40 differed in the ability to induce**
1160 **antibodies against spirochetes in robin and white-footed mice during infection.** *Ixodes*
1161 *scapularis* nymphs infected with *B. burgdorferi* B31-5A4, 297, or cN40, or naïve nymphs
1162 (Uninfect.) were allowed to feed to repletion on **(A to E)** American robins or **(F to J)** white-footed
1163 (WF) mice. The sera were obtained at **(A and F)** 0-, **(B and G)** 7-, **(C and H)** 14-, **(D and I)** 21-,
1164 or **(E and J)** 28-days post nymph feeding ("dpf"). The levels of IgG against the mixture of *B.*
1165 *burgdorferi* strains B31-5A4, 297, and cN40 (1×10^6 spirochetes per strain in each microtiter well)
1166 were determined using quantitative ELISA. Shown are the geometric mean ± geometric standard
1167 deviation of five white-footed mice or robins per group (3, 4, 5, and 4 for the strains B31-5A4-,
1168 297-, cN40-infected robins or uninfected robins per group, respectively). Significant differences
1169 ($p < 0.05$) in the antibody titers relative to robins or white-footed mice fed on by naive nymphs
1170 (''*'') are indicated. Sera from the **(K)** American robins and **(L)** white-footed (WF) mice at 7 days
1171 after fed on by *I. scapularis* nymphs carrying *B. burgdorferi* strains B31-5A4, 297, or cN40, or
1172 naïve nymphs (Uninfect.) were collected. These sera were serially diluted as indicated and mixed
1173 with **(K)** chicken or **(L)** guinea pig complement and the mixture of the strains B31-5A4, 297, and
1174 cN40 (1×10^7 spirochetes per strain in each reaction). After incubation for 24 h, surviving
1175 spirochetes were quantified from three fields of view for each sample microscopically. The
1176 experiment was performed at three independent occasions. The survival percentage was derived
1177 from the proportion of serum-treated to untreated spirochetes. Data shown are the mean ± standard
1178 error of the mean (SEM) of the survival percentage from three replicates in one representative
1179 experiment. The 50% borreliacidal dilution of each serum sample (50% BA), representing the
1180 dilution rate that effectively killed 50% of spirochetes, was obtained from curve-fitting and
1181 extrapolation of data shown in the table above respective panels. The 50% BA of some strain-sera

1182 pairs could not be determined because no robust killing was observed, resulting in curves that did
1183 not fit (N.F.).
1184
1185 **Figure 7. The schematic diagram showing the model supported by this study.** Upon *B.*
1186 *burgdorferi* transmission from ticks to hosts, multiple cellular and immunological mechanisms
1187 may play in concert to determine the fitness of spirochetes in hosts. These mechanisms include the
1188 ability of *B. burgdorferi* to attach to cells or tissues (spirochete adhesiveness) and escape from host
1189 immune clearance (early host defense), such as complement, cytokine-mediated responses, and
1190 antibodies. Both mechanisms applied on spirochetes would lead to host specialization, resulting in
1191 the association of *B. burgdorferi* with particular hosts (i.e. mammal or avian specialists).
1192
1193
1194
1195
1196
1197
1198
1199
1200
1201
1202
1203
1204

Fig. 1

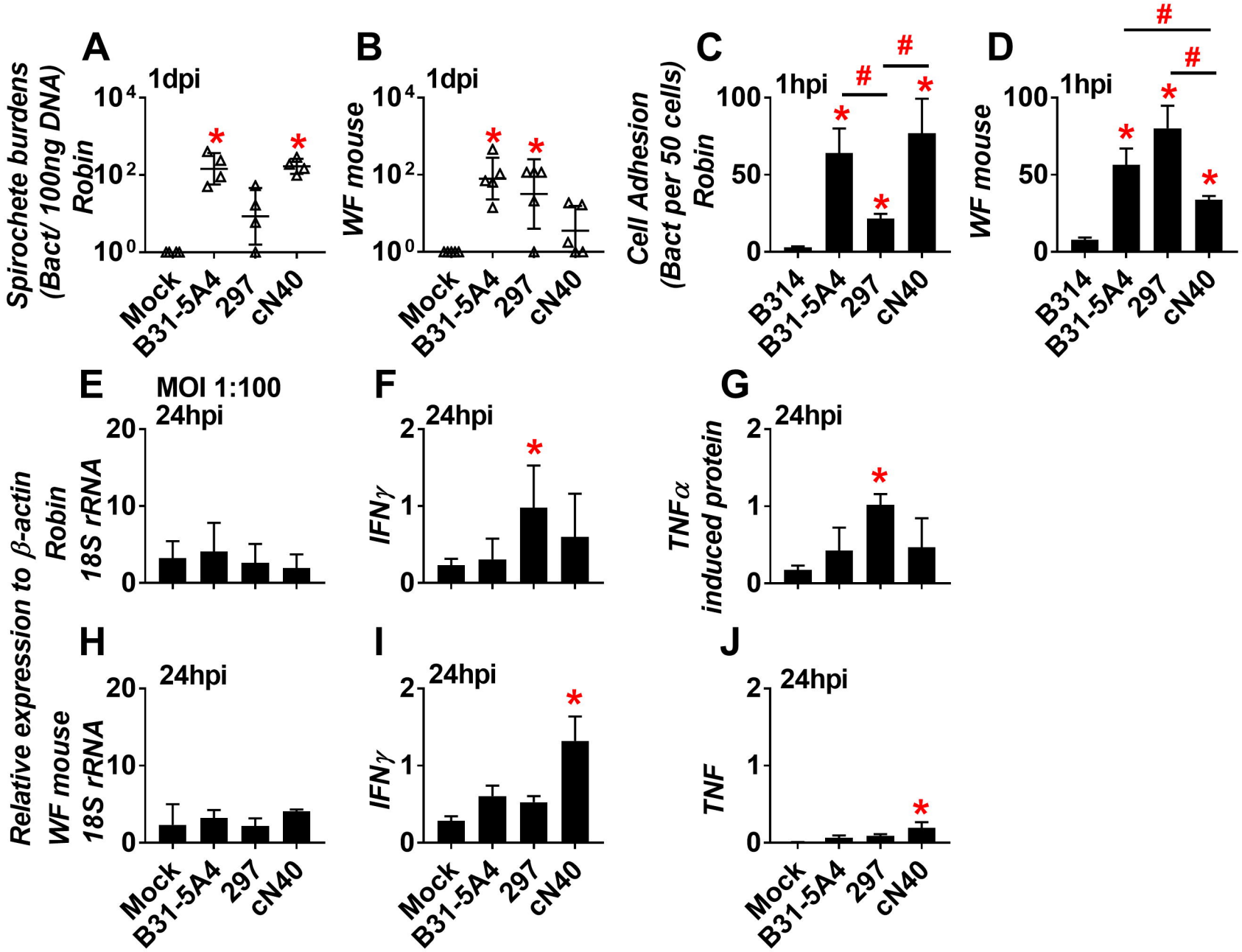
A
1dpi
Spirochete burdens (Bact/ 100ng DNA)
Robin
10^4
10^2
10^0
Mock
B31-5A4
297
cN40
B
1dpi
WF mouse
10^4
10^2
10^0
Mock
B31-5A4
297
cN40
C
1hpi
Cell Adhesion (Bact per 50 cells)
Robin
100
50
0
B314
B31-5A4
297
cN40
D
1hpi
WF mouse
100
50
0
B314
B31-5A4
297
cN40
E
MOI 1:100
24hpi
Relative expression to β-actin
Robin
18S rRNA
20
10
0
F
24hpi
IFNγ
2
1
0
G
24hpi
TNFα induced protein
2
1
0
H
24hpi
WF mouse
18S rRNA
20
10
0
Mock
B31-5A4
297
cN40
I
24hpi
IFNγ
2
1
0
Mock
B31-5A4
297
cN40
J
24hpi
TNF
2
1
0
Mock
B31-5A4
297
cN40

Fig. 2

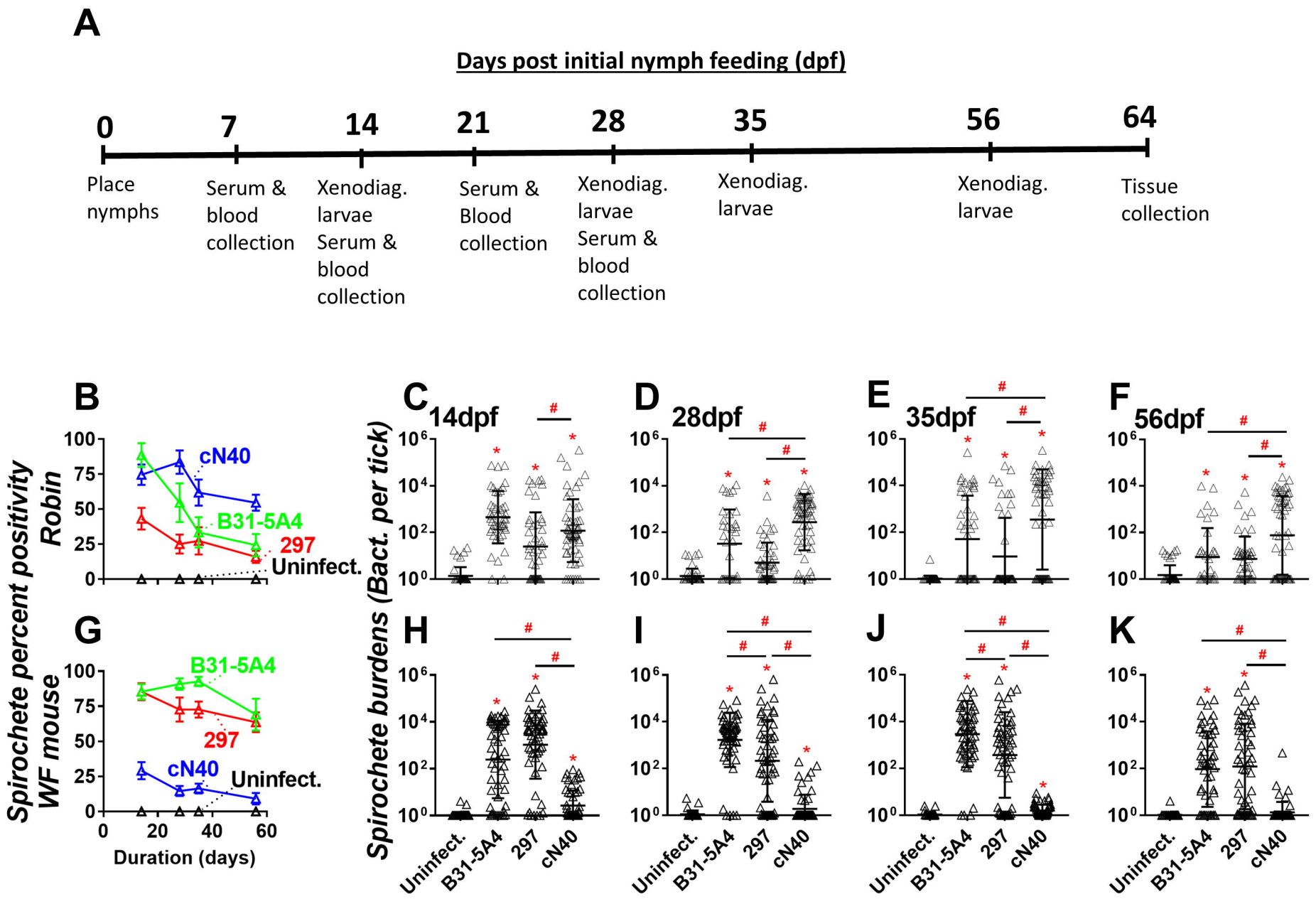
A
Days post initial nymph feeding (dpf)
0
7
14
21
28
35
56
64
Place nymphs
Serum & blood collection
Xenodiag. larvae Serum & blood collection
Serum & Blood collection
Xenodiag. larvae Serum & blood collection
Xenodiag. larvae
Xenodiag. larvae
Tissue collection
B
Spirochete percent positivity Robin
cN40
B31-5A4
297
Uninfect.
G
Spirochete percent positivity WF mouse
B31-5A4
297
cN40
Uninfect.
Duration (days)
C 14dpf
D 28dpf
E 35dpf
F 56dpf
H
I
J
K
Spirochete burdens (Bact. per tick)
Uninfect.
B31-5A4
297
cN40

Fig. 3

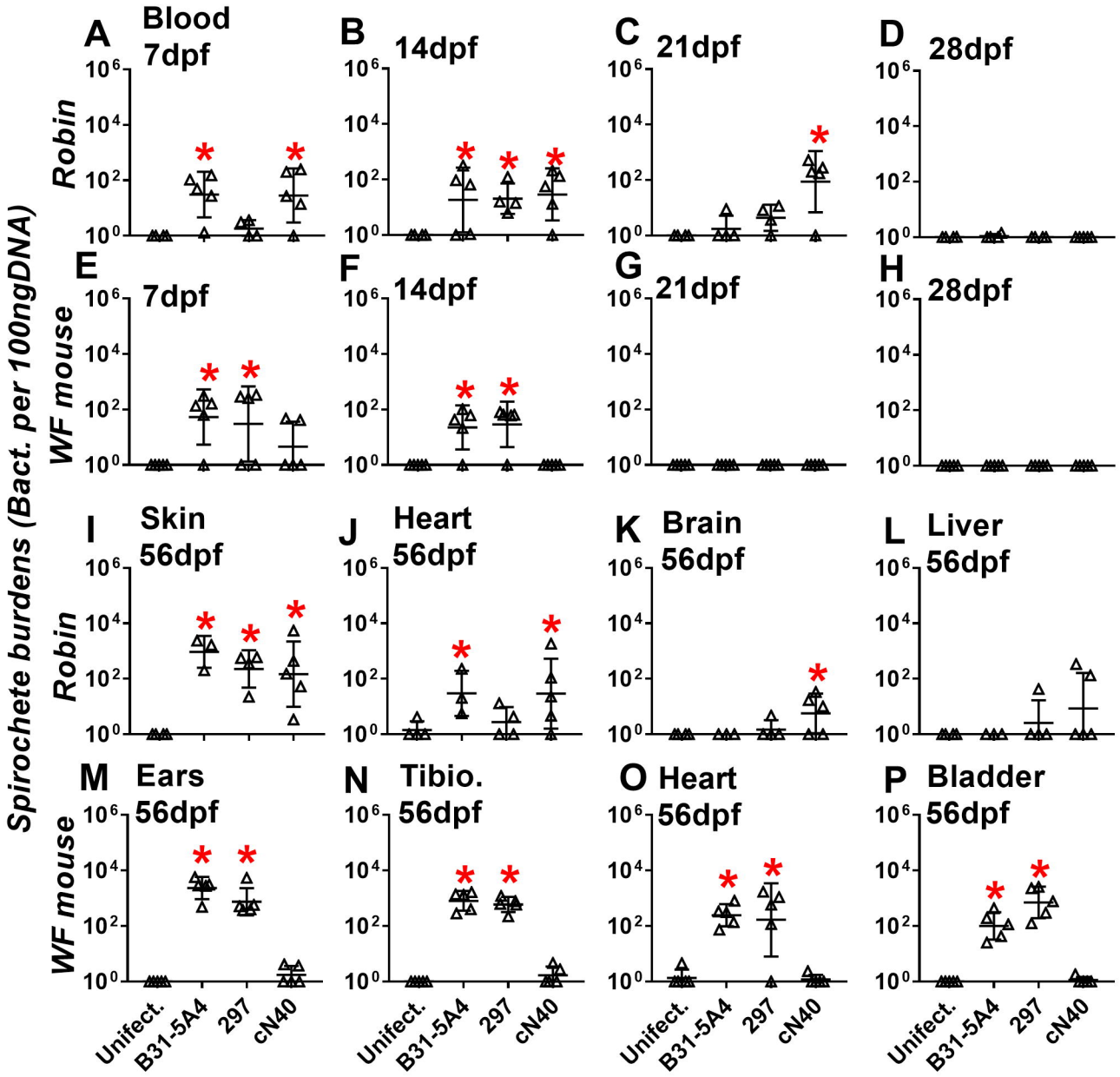
Spirochete burdens (Bact. per 100ngDNA)
A Blood 7dpf
B 14dpf
C 21dpf
D 28dpf
E 7dpf
F 14dpf
G 21dpf
H 28dpf
I Skin 56dpf
J Heart 56dpf
K Brain 56dpf
L Liver 56dpf
M Ears 56dpf
N Tibio. 56dpf
O Heart 56dpf
P Bladder 56dpf
Robin
WF mouse
10^6
10^4
10^2
10^0
Unifect.
B31-5A4
297
cN40

Fig. 4

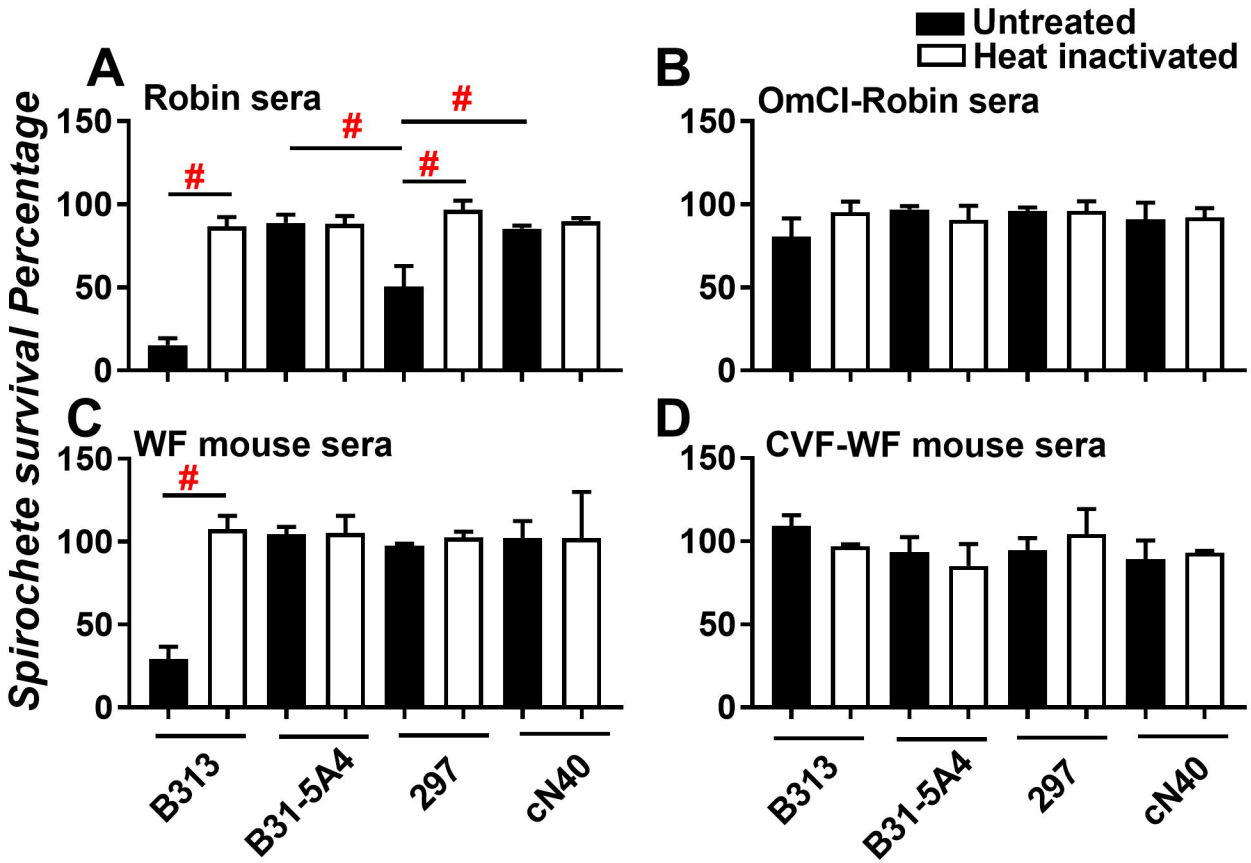
Untreated
Heat inactivated
A
Robin sera
B
OmCI-Robin sera
C
WF mouse sera
D
CVF-WF mouse sera
Spirochete survival Percentage
150
100
50
0
#
B313
B31-5A4
297
cN40

Fig. 5

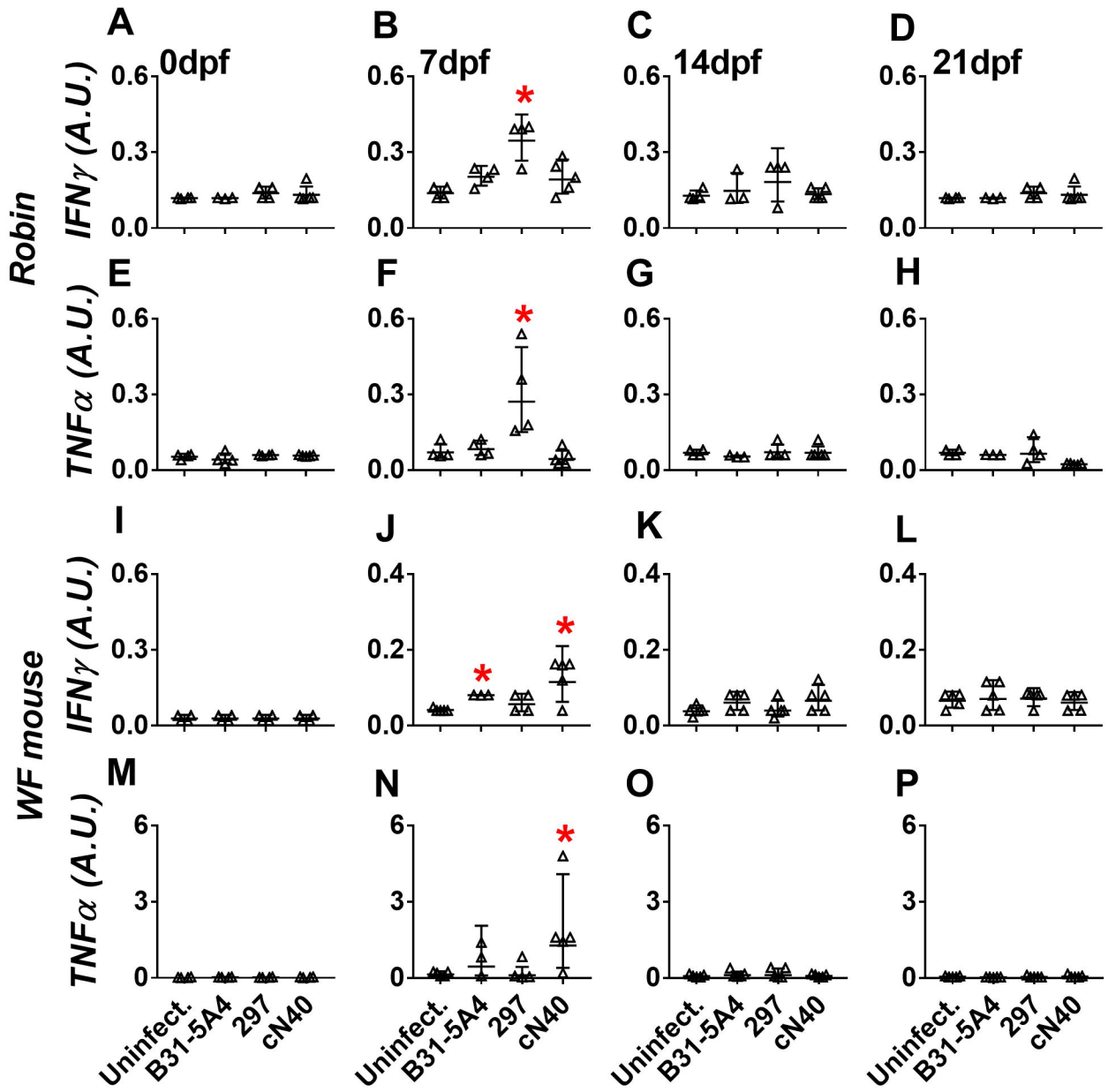
A
0dpf
B
7dpf
C
14dpf
D
21dpf
E
F
G
H
I
J
K
L
M
N
O
P
Robin
WF mouse
IFNγ (A.U.)
TNFα (A.U.)
0.6
0.3
0.0
0.4
0.2
6
3
0
*
Uninfect.
B31-5A4
297
cN40

Fig. 6

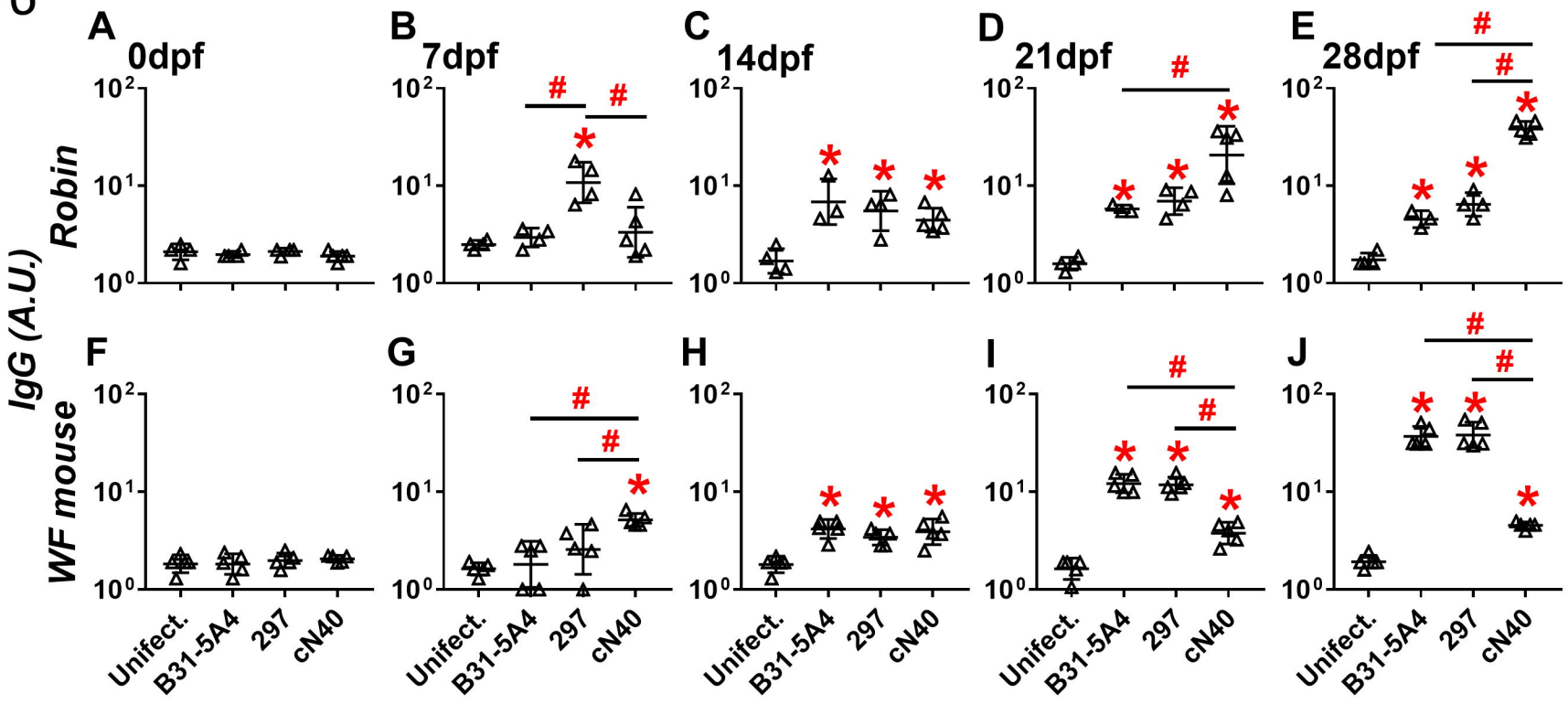

K

	Sera from Robins infected with			
	B31-5A4	297	cN40	Uninfect.
50%BA	N.F.	52±2	N.F.	N.F.

L

	Sera from WF mice infected with			
	B31-5A4	297	cN40	Uninfect.
50%BA	N.F.	N.F.	32±4	N.F.

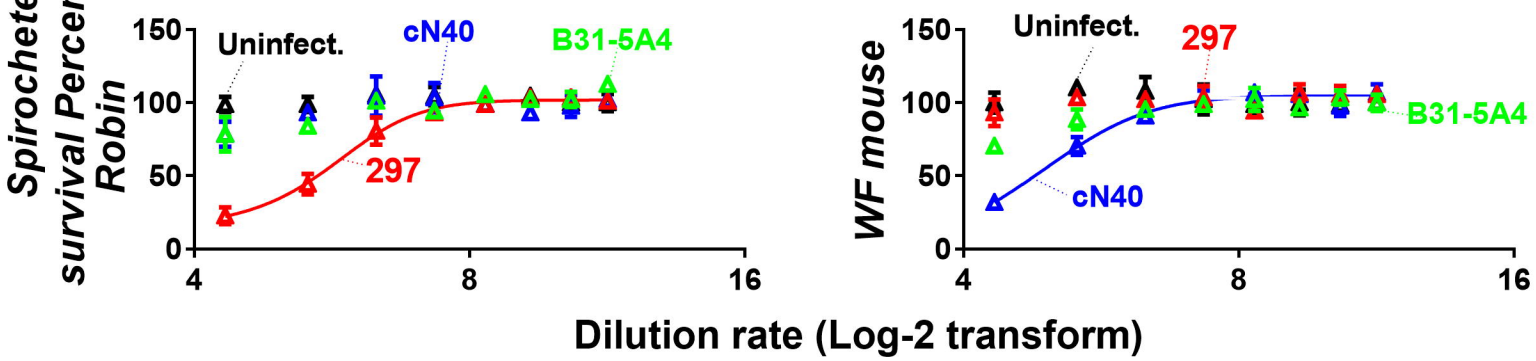

Fig. 7

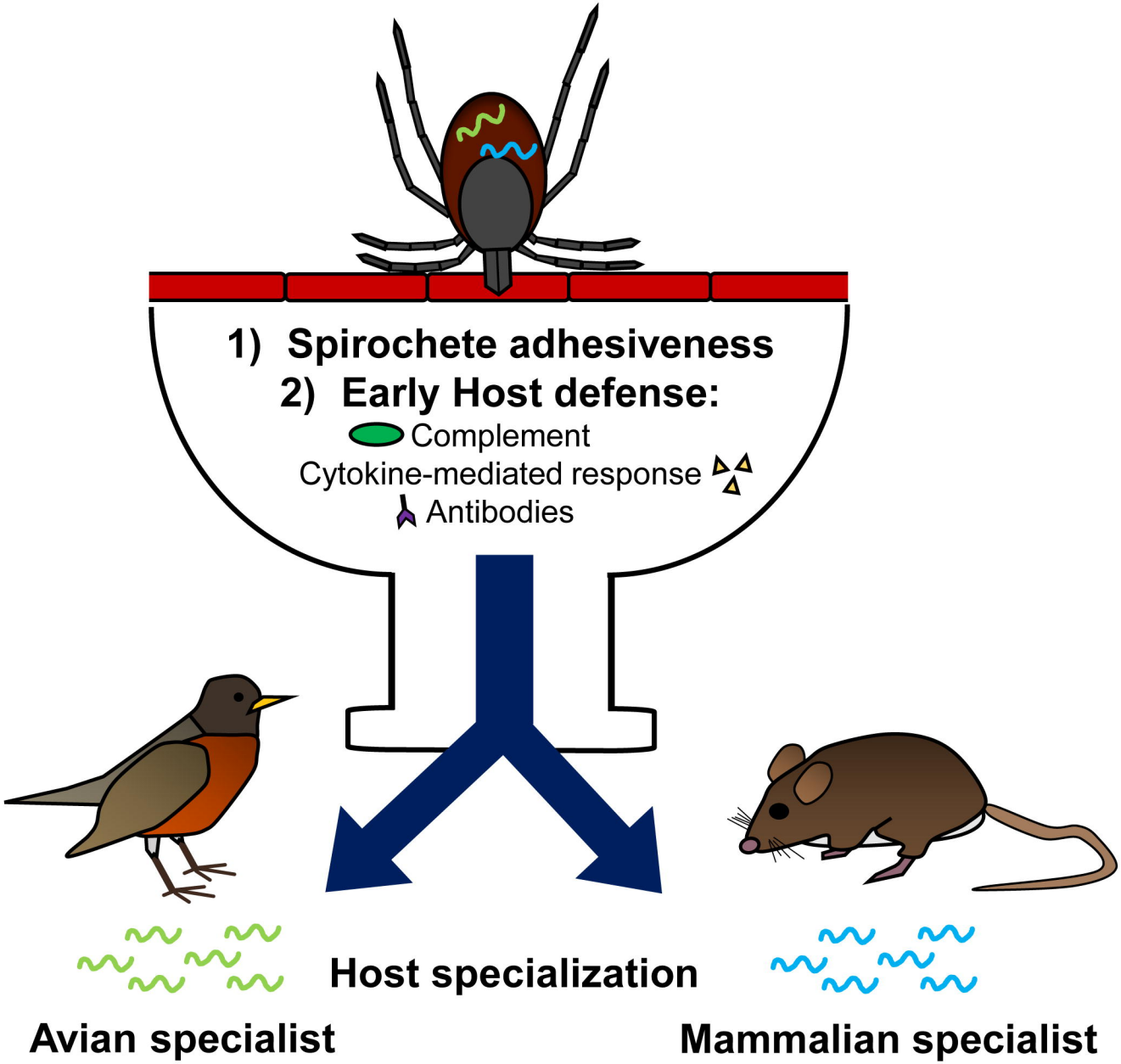
1) Spirochete adhesiveness
2) Early Host defense:
Complement
Cytokine-mediated response
Antibodies
Host specialization
Avian specialist
Mammalian specialist